A peer-reviewed version of this preprint was published in PeerJ on 20 January 2020.

View the peer-reviewed version (peerj.com/articles/8303), which is the preferred citable publication unless you specifically need to cite this preprint.

Paffendorf BAM, Qassrawi R, Meys AM, Trimborn L, Schrader A. 2020. TRANSPARENT TESTA GLABRA 1 participates in flowering time regulation in *Arabidopsis thaliana*. PeerJ 8:e8303 https://doi.org/10.7717/peerj.8303

Initial embedding of TRANSPARENT TESTA GLABRA 1 in the *Arabidopsis thaliana* flowering time regulatory pathway

Barbara A M Paffendorf [1], **Rawan Qassrawi** [1], **Andrea M Meys** [1], **Laura Trimborn** [1], **Andrea Schrader** [Corresp. 1]

[1] Botanical Institute, Department of Biology, University of Cologne, Cologne, Germany

Corresponding Author: Andrea Schrader
Email address: Andrea.Schrader@uni-koeln.de

Pleiotropic regulatory factors mediate concerted responses of the plant's trait network to endogenous and exogenous cues. TRANSPARENT TESTA GLABRA 1 (TTG1) is a pleiotropic regulator that has been predominantly described in its role as a regulator of early accessible developmental traits. Although its closest homologs LIGHT-REGULATED WD1 (LWD1) and LWD2 are regulators of photoperiodic flowering, a role of TTG1 in flowering time regulation has not been reported.

Here we reveal that TTG1 is a regulator of flowering time in Arabidopsis thaliana and changes transcription levels of different targets within the flowering time regulatory pathway. *TTG1* mutants flower early and TTG1 overexpression lines flower late at long-day conditions. Consistently, TTG1 can suppress the transcript levels of the floral integrators *FLOWERING LOCUS T* and *SUPPRESSOR OF OVEREXPRESSION OF CO1* and can act as an activator of circadian clock components. Moreover, TTG1 might form feedback loops at the protein level. The TTG1 protein interacts with PSEUDO RESPONSE REGULATOR (PRR)s and basic HELIX-LOOP-HELIX 92 (bHLH92) in yeast. *In planta*, the respective pairs exhibit interesting patterns of localization including a recruitment of TTG1 by PRR5 to subnuclear foci. This mechanism proposes additional layers of regulation by TTG1 and might aid to specify the function of bHLH92.

Within another branch of the pathway, TTG1 can elevate *FLOWERING LOCUS C* (*FLC*) transcript levels. FLC mediates signals from the vernalization, ambient temperature and autonomous pathway and the circadian clock is pivotal for the plant to synchronize with diurnal cycles of environmental stimuli like light and temperature. Our results suggest an unexpected positioning of TTG1 upstream of *FLC* and upstream of the circadian clock. In this light, this points to an adaptive value of the role of TTG1 in respect to flowering time regulation.

Initial embedding of TRANSPARENT TESTA GLABRA 1 in the *Arabidopsis thaliana* flowering time regulatory pathway

Barbara A. M. Paffendorf[1], Rawan Qassrawi[1], Andrea M. Meys[1], Laura Trimborn[1], Andrea Schrader[1]

[1] Botanical Institute, Department of Biology, University of Cologne, Cologne, Germany

Corresponding Author:
Andrea Schrader[1]
Email address: Andrea.Schrader@uni-koeln.de

Abstract

Pleiotropic regulatory factors mediate concerted responses of the plant's trait network to endogenous and exogenous cues. TRANSPARENT TESTA GLABRA 1 (TTG1) is a pleiotropic regulator that has been predominantly described in its role as a regulator of early accessible developmental traits. Although its closest homologs LIGHT-REGULATED WD1 (LWD1) and LWD2 are regulators of photoperiodic flowering, a role of TTG1 in flowering time regulation has not been reported.

Here we reveal that TTG1 is a regulator of flowering time in Arabidopsis thaliana and changes transcription levels of different targets within the flowering time regulatory pathway. *TTG1* mutants flower early and TTG1 overexpression lines flower late at long-day conditions. Consistently, TTG1 can suppress the transcript levels of the floral integrators *FLOWERING LOCUS T* and *SUPPRESSOR OF OVEREXPRESSION OF CO1* and can act as an activator of circadian clock components. Moreover, TTG1 might form feedback loops at the protein level. The TTG1 protein interacts with PSEUDO RESPONSE REGULATOR (PRR)s and basic HELIX-LOOP-HELIX 92 (bHLH92) in yeast. *In planta*, the respective pairs exhibit interesting patterns of localization including a recruitment of TTG1 by PRR5 to subnuclear foci. This mechanism proposes additional layers of regulation by TTG1 and might aid to specify the function of bHLH92.

Within another branch of the pathway, TTG1 can elevate *FLOWERING LOCUS C* (*FLC*) transcript levels. FLC mediates signals from the vernalization, ambient temperature and autonomous pathway and the circadian clock is pivotal for the plant to synchronize with diurnal cycles of environmental stimuli like light and temperature. Our results suggest an unexpected positioning of TTG1 upstream of *FLC* and upstream of the circadian clock. In this light, this points to an adaptive value of the role of TTG1 in respect to flowering time regulation.

Introduction

While a species adapts to ranges of abiotic and biotic conditions, the individual plant must cope with its daily local conditions. It achieves this by integrating various signaling pathways and the current status of the plant itself - for example its developmental stage or the combination and availability of metabolites. Pleiotropic regulators aid in concerted responses and, thereby, regulate a subset of the plant's trait network. Due to the depth of insights achieved in the past decades of plant molecular biology, its model species *Arabidopsis thaliana* (*A. thaliana*) (Koornneef & Meinke 2010) is well suited to analyze such pleiotropic regulators.

TRANSPARENT TESTA GLABRA 1 (TTG1) is one such pleiotropic regulator. It is known as the head of an evolutionarily conserved gene regulatory network that controls five major TTG1-dependent traits of adaptive value: seed pigmentation (production of proanthocyanidin), accumulation of anthocyanidins (in seedlings), seed coat mucilage production, trichome and root hair patterning (Zhang et al. 2003).
Molecular mechanisms underlying these early (accessible) developmental traits are under investigation since decades in *A. thaliana* and beyond. Already in 1981, the *ttg1* syndrome was described for induced *A. thaliana* mutants comprising yellow seeds having a transparent testa, the absence of trichomes (glabrous leaves), the absence of anthocyanidin accumulation and the absence of seed mucilage (Koornneef 1981).

TTG1 is expressed in all major organs of *A. thaliana* including the meristem (Walker et al. 1999). Analysis of flower buds from Col-0 and *ttg1-9* mutants revealed a similar transcript level of *TTG1* and *TTG1-9* (Walker et al. 1999). In the same tissue, *TTG1-11* transcript levels are higher than those of *TTG1* from Col-0 and the *TTG1-10* (Ws) transcript is almost absent as compared to Col-0 (Larkin et al. 1999). The gene encodes a WD40 repeat protein (Walker et al. 1999). The integrity of its WD40 repeats is crucial to its function and its C- terminus is expected to be of high relevance for the protein's proper folding and domain structure (Zhang & Schrader 2017).

Basic HELIX-LOOP-HELIX (bHLH) and MYELOBLASTOSIS (MYB) factors contribute with differing specificity to the respective TTG1-dependent trait regulation for which they form R2R3MYB-bHLH-WD40 (MBW) complexes with TTG1 (Balkunde et al. 2010; Broun 2005; Koornneef 1981; Lepiniec et al. 2006; Miller et al. 2015; Ramsay & Glover 2005; Tominaga-Wada et al. 2011; Walker et al. 1999). The classical bHLH factors from the TTG1-network - GLABRA 3 (GL3), ENHANCER OF GL3 (EGL3), TANSPARENT TESTA 8 (TT8) and MYC1 - interact with TTG1 and different R2R3-MYB transcription factors (Zhang & Schrader 2017). Multilayered regulatory mechanisms have been described for TTG1 like differential complex composition, competitive scenarios, movement, trapping to the nucleus and mutual localization

with respective interactors (Balkunde et al. 2011; Bouyer et al. 2008; Pesch et al. 2013; Pesch et al. 2015; Wester et al. 2009; Zhang et al. 2019; Zhang et al. 2003; Zhao et al. 2008).

Few additional traits like the carbon partitioning between seed oil, seed pigment and seed mucilage biosynthesis pathway were analyzed in dependence of TTG1 (Chen et al. 2015; Li et al. 2018). However, surprisingly little is known about the role of TTG1 towards late developmental traits.

One of the most important developmental switches in the plant's life cycle is the transition from vegetative to reproductive phase. The appropriate regulation of flowering time is essential for the reproductive success of plants and therefore a key determinator of plant fitness.

Several genetically identified pathways that are involved in the regulation of flowering time are influenced by environmental (e.g. vernalization, ambient temperature and photoperiod) and endogenous (e.g. autonomous, gibberellin, circadian clock, age, sugar budget) signals (Blumel et al. 2015). These interwoven regulatory mechanisms converge to the floral integrators *FLOWERING LOCUS T* (*FT*), *SUPPRESSOR OF OVEREXPRESSION OF CO1* (*SOC1*) and also *LEAFY* (*LFY*) (Simpson & Dean 2002).

CONSTANS (CO) and FT form an important module of the photoperiodic pathway. *CO* expression rises about 8h after dawn with a peak at night (Suarez-Lopez et al. 2001). The accumulating CO protein activates the florigen gene *FT* in leaves (An et al. 2004; Song et al. 2015). In the night, CO is degraded through the COP1/SPA complex (CONSTITUTIVE PHOTOMORPHO-GENESIS 1/SUPPRESSOR OF PHYA-105) (Jang et al. 2008; Laubinger et al. 2006; Liu et al. 2008). Hence, at long days, sufficient FT protein is formed in the leaves and moves to the shoot apical meristem where it induces flowering (Andres & Coupland 2012). Although *CO* is expressed under short-day (SD) conditions, it cannot sufficiently induce *FT* expression due to the extended night (Valverde et al. 2004). Consequently, mutants of the photoperiod pathway flower late under long-day (LD) conditions and do not deviate in flowering time from the wild type at SD conditions. One such mutant is the *gigantea* (*gi*) mutant. GI is an activator of CO (Sawa et al. 2007). Its protein levels are also regulated by COP1 in presence of EARLY FLOWERING 3 (ELF3) (Yu et al. 2008).

A. thaliana is a facultative LD plant. Winter annual accessions flower late and are responsive to vernalization which reduces the FRIGIDA (FRI)-activated transcript levels of the floral repressor *FLOWERING LOCUS C* (*FLC*) through epigenetic modifications at the *FLC* locus (Deng et al. 2018; Hepworth & Dean 2015). In the rapid-cycling summer annual accessions, either *FRI* is defective, which reduces *FLC* transcript levels, or the *FLC* allele is weak (Michaels et al. 2003). Low levels of FLC induce flowering as FLC is a suppressor of *FT* (Searle et al. 2006). FT activates the downstream transcription factors *LEAFY* (*LFY*) and *APETALA1* (*AP1*) at the shoot

apical meristem and thereby causes flowering when an FT threshold is passed (Turck et al. 2008).

SOC1 acts downstream of *FT* and upstream of *LFY*. It is similarly as *FT* directly targeted by the floral repressor FLC (Lee & Lee 2010) which mediates signals from the autonomous and vernalization response pathways. Both pathways act through suppression of *FLC* expression (Simpson & Dean 2002). SHORT VEGETATIVE PHASE (SVP) is an interaction partner of FLC (Li et al. 2008) and both are mediators of the ambient temperature pathway (Lee et al. 2007; Simpson & Dean 2002). Ambient temperature adjusts flowering time in a way that cool temperature delays flowering, whereas warm temperature accelerates flowering (Balasubramanian et al. 2006; Blazquez et al. 2003). SVP itself also acts as a direct suppressor of *FT* and *SOC1* (Li et al. 2008). Moreover, SVP can activate members of a group of additional *FT* suppressors, the APETALA2 (AP2) domain containing transcription factors TEMPRANILLO (TEM) 1 and TEM2 (RAV transcription factors with AP2/ERF and B3 DNA -binding domain), AP2 and the AP2-like transcription factors SCHLAFMÜTZE (SMZ), SCHNARCHZAPFEN (SNZ), TARGETs OF EARLY ACTIVATION TAGGED (EAT) (TOE) 1, TOE2 and TOE3 (Tao et al. 2012; Yant et al. 2009). These AP2 domain containing factors act directly at the *FT* gene. TOE1 is able to bind to the *FT* promoter close to the CO-binding site (Zhang et al. 2015). SMZ also seems to effect *FT* expression directly, since *FT* was found as a target of SMZ in a ChIP-chip assay (Mathieu et al. 2009). TEM1 and TEM2 act as *FT* repressors by binding to its 5′UTR. Furthermore, it is suggested that the balance between TEM and CO controls *FT* transcription and thereby is involved in determination of flowering (Castillejo & Pelaz 2008).

The AP2 domain containing factors are not only connected with the ambient temperature pathway but also with the gibberellin signaling pathway by TEM1 and TEM2 (Osnato et al. 2012). Moreover, TOE1 interacts with the activating region of CO and the LOV domain of FLAVIN-BINDING KELCH REPEAT F-BOX1 (FKF1). This prevents CO from activating *FT* transcription and FKF1 from stabilizing CO (Zhang et al. 2015).

Upstream of CO, the circadian clock influences the flowering time regulatory pathway. Circadian oscillators are the key for a plant to synchronize with the external environmental cues providing an adaptive advantage (Dodd et al. 2005; Michael et al. 2003). The circadian clock and its feedback loops cause in general rhythmic gene expression within and downstream of the clock. A screen analyzing the MYB BHLH and bZIP factors in *A. thaliana* found that 20% of these are under the control of the clock (Hanano et al. 2008). MYB3R2, bHLH69 and bHLH92 were found to in turn alter clock parameters when overexpressed and therefore might position upstream of the clock (Hanano et al. 2008).

The core negative feedback loop of the clock is formed by the MYB-like proteins CIRCADIAN CLOCK ASSOCIATED 1 (CCA1) and LATE ELONGATED HYPOCOTYL (LHY) which are expressed in the morning and the evening expressed PSEUDO RESPONSE REGULATOR

(PRR) PRR1/ TIMING OF CAB EXPRESSION 1 (TOC1) (Oakenfull & Davis 2017). Several additional loops are formed within the central oscillator. *PRR9*, *PRR7*, *PRR5* and *PRR3* peak successively during the day (Matsushika et al. 2000) filling the gap between *CCA1*/*LHY* and *TOC1*. The PRRs act as suppressors of *CCA1* and *LHY* (Nakamichi et al. 2010). Moreover, GI forms a predicted feedback loop with TOC1 (Locke et al. 2006) and the evening complex consisting of ELF4, ELF3 and LUX ARRHYTHMO (LUX) is required to maintaining circadian rhythms through regulating different key clock genes (Huang & Nusinow 2016).

The PRR proteins have an N-terminal pseudo-receiver domain which is similar to the phospho-accepting receiver of the two-component response regulators but lacks the presumed phosphor-accepting aspartate. At their C-terminus, a CO, CO-like and TOC1 (CCT) motif is shared by the name-giving proteins (Makino et al. 2000; Matsushika et al. 2000; Strayer et al. 2000). *PRR*s act antagonistically with *LHY/CCA1* on the downstream CO-FT module (Nakamichi et al. 2007). At the protein level, PRRs interact with and stabilize the CO protein enhancing CO-mediated *FT* transcription (Hayama et al. 2017).

Only few transcriptional activators of the circadian clock are known (Shim et al. 2017). One of these is LIGHT-REGULATED WD1 (LWD1). LWD1 and LWD2 are the closest homologs of TTG1 that regulate photoperiodic flowering (Wu et al. 2008). Double mutants flower early at LD conditions and exhibit increased *FT* transcript levels (Wu et al. 2008). The *LWD* genes are rhythmically expressed in dependence of PRR9 which forms a feed-back loop with LWD1 (Wang et al., 2011). LWD1 can bind to the promoter of *PRR5*, *PRR9* and *PRR1/TOC1*. With TEOSINTE BRANCHED1-CYCLOIDEA-PCF20 (TCP20) and TCP22 it binds to the *CCA1* promoter activating its expression (Wang et al. 2011; Wu et al. 2016). To date, there was no evidence suggesting an involvement of TTG1 in the regulation of the circadian clock and flowering time. A potential involvement of TTG1 in its transcriptional control has not been reported.

Here we reveal that TTG1 can modulate flowering time along with an initial embedding of TTG1 in the flowering time regulatory pathway. Most strikingly, TTG1 can suppress *FT* and *SOC1* transcript levels and increase those of clock components while reducing their amplitude as observed within one day. PRR proteins can interact with TTG1 in yeast and exhibit interesting subcellular localization patterns of and with TTG1 when co-expressed *in planta*. In the same systems, TTG1 also interacts with and modulates the localization of bHLH92. Flowering time results at LD conditions and the integrators' transcript levels are in line with an increase of the *FLC* transcript level upon TTG1 overexpression. Together, at the molecular level, we suggest that TTG1 acts in multilayered regulatory processes in flowering time regulation and it might act upstream of FLC and the clock.

Materials & Methods

Plant material und growth conditions. The used *A. thaliana* mutants *ttg1-9*, *ttg1-11*, *ttg1-21*, *ttg1-22*, *gl3-3*, *egl3-19114*, *tt8-SALK*, *myc1-1*, *cop1-4* (all Col-0), *ttg1-1* (L*er*), *ttg1-10* (Ws) (Table S7) have been described before (Alonso et al. 2003; Appelhagen et al. 2014; Jakoby et al. 2008; Koornneef 1981; Larkin et al. 1994; Larkin et al. 1999; McNellis et al. 1994; Pesch et al. 2013; Rosso et al. 2003; Walker et al. 1999; Wester et al. 2009). Primers including dCAPS primers (Appelhagen et al. 2011; Jaegle et al. 2016; Neff et al. 2002; Schrader et al. 2013) used for genotyping of mutants can be found in Table S8. The floral dip method (Clough & Bent 1998) was used to generate overexpression lines in Col-0 and *cop1-4* background. T_1 plants were BASTA selected and resistant plants were screened for YFP fluorescence using a Leica stereomicroscope (MZ FLIII) (Leica Microsystems, www.leica-microsystems.com). This analysis was repeated for plants homozygous for the insert being at least in T_3 generation and overexpressing YFP-TTG1 (Table S4). Two walk-in plant chambers were used. Detailed conditions at the respective used areas are listed in Table S1. For flowering time experiments, single seeds were placed in parallelly prepared pots with soil and stratified for 7 d at 5°C before being transferred to the respective growth condition.

Seedlings for qRT-PCR experiments were sterilized with 70% (v/v) ethanol, 2% NaOCl, stratified at 5°C and grown on Murashige and Skoog medium containing 1% sucrose at "cold" LD conditions (see Table S1). Seedlings for circadian transcript profiles were snap frozen in liquid nitrogen (~100 mg) on day eight starting at ZT0 in 4h intervals until ZT20. Samples used comparing transcript levels in the overexpression lines OE01-03 and OE19-21 were similarly harvested at ZT11 and ZT13 as well as parallelly grown seedlings for comparing protein levels in the same lines at ZT11 and ZT10, respectively. Three biological replicates were analyzed for circadian profiles and comparisons of transcript and protein levels among the TTG1 overexpression lines.

Phenotyping. Flowering time was recorded as the number of post-stratification days until bolting and the total number of leaves at the time point of bolting. Bolting was defined as the time at which the first bud was visible. Two (bHLH overexpression lines' experiment) or three experiments (TTG1 overexpression lines, all *ttg1* mutant sets) were conducted for each set of analyzed genotypes and for each condition with at least six individual plants per genotype and experiment. See Table S2 for details.

Constructs. Gateway™ (Invitrogen™, www.invitrogen.com) entry clones containing the coding DNA sequence (CDS) for the respective protein were generated using BP reaction with the previously published vectors *TTG1*pAS2.1 and *GL3*pcACT2 (Pesch et al. 2015), *EGL3*pcACT2, *TT8*pAS2.1, *MYC1*pAS2.1 (vectors provided by M. Pesch) or PCR products using primers for *TOC1*, *PRR5*, *PRR7*, *PRR9*, *bHLH92*, *LWD1* and *LWD2* CDS are listed in Table S8 and cDNA from Col-0 seedlings as a template or using the vectors 35S::PRR7:CFP and 35S::PRR9:CFP (Hayama et al. 2017) as a template, respectively. The used entry vector in all cases was pDONR207 (Invitrogen). All entry vectors were sequenced. To generate the construct used for

the overexpression lines OE01-03 in Col-0 and OE19-OE21 in *cop1-4* background, *TTG1*pDONR207 was recombined using Gateway™ LR Clonase™ (Invitrogen™) into pENSG-YFP (N. Medina-Escobar, a version for C-terminal fusions was published before (Feys et al. 2005)). In analogy, the CDS in pDONR207 for *GL3* (OE04-OE06), *EGL3* (OE07-OE09), *TT8* (OE10-OE12) and *MYC1* (OE13-OE15) were recombined into pENSG-YFP and used to generate the overexpression lines numbered as given in brackets and expressing YFP-bHLH fusion proteins driven by the Pro35s.
For tobacco co-localization experiments, *TTG1*pDONR207 and *PRR5*pDONR207 were recombined into pNmR (Schrader et al. 2013) and *PRR5*, *PRR7*, *PRR9*, *TOC1*, *bHLH92* (all in pDONR207) were recombined into pENSG-CFP (N. Medina-Escobar, a version for C-terminal fusions was published before (Feys et al. 2005)) and for the Y2H experiments, also in pAS2.1-attR and pACT-attR (Clontech, www.clontech.com, modified J.F. Uhrig). *LWD1*pDONR207 and *LWD2*pDONR207 were similarly used in combination with pAS2.1-attR and pACT-attR.
In analogy to YFPattB1-pBat-TL-B-p35s and RFP-HAattB1-pBat-TL-B-p35s previously created as negative controls (Schrader et al. 2013) CFPattB1 was amplified from pENSG-CFP with primers ANS393 and ANS235 and recombined in pBat-TL-B-p35s (Schrader et al. 2013) to obtain CFPattB1-pBat-TL-B-p35s.

qRT-PCR experiments. About 100 mg of seedlings was harvested for each RNA extraction. RNA extractions were done according to the manufacturer's instructions (RNeasy Plant Mini Kit, Qiagen, www.qiagen.com) using a Tissue Lyser (Qiagen) and followed by DNase I (ThermoFisher, https://www.thermofisher.com) treatment. RNA integrity was tested on a gel prior to cDNA synthesis (SuperScript™ III First-Strand Synthesis System, Invitrogen, or the RevertAid First Strand cDNA Synthesis Kit, ThermoFisher) and RNaseH treatment as suggested before (Martel et al. 2002). A PCR using Elongation factor 1-alpha 1 (EF1ALPHA) primers (Kirik et al. 2007) spanning an intron served as a control to ensure that there was no genomic DNA in the cDNA synthesis (Primers in Table S8).
qRT-PCR was performed using the QuantStudio 5 Real-Time PCR Systems (ThermoFisher) with POWER SYBR Green PCR-Master Mix (Applied Biosystems), the respective cDNA and gene-specific primers. *UBQ10* (*UBIQUITIN10*) was used as a reference gene (Harari-Steinberg et al. 2001; Sun & Callis 1997). Three biological replicates with three technical replicates each were performed. Calculations are described in detail in Table S3 and Table S5. All used primers are listed in Table S8. Most of these were described before (Grigorova et al. 2011; Hayama et al. 2017; Li et al. 2008; Maier et al. 2013; Nakamichi et al. 2007; Shin et al. 2017; Wang et al. 2014; Wang et al. 2011; Wenden et al. 2011; Yu et al. 2012; Zhang et al. 2015; Zou et al. 2013).
For TTG1 endo, TTG1 both and TTG1 no LWD see Fig. 1G and Fig. S2.

Comparison of protein levels. Samples were homogenized under liquid nitrogen to compare YFP-tagged TTG1 in the overexpression lines OE01-03 and OE19-21. 150 µl of lysis buffer (Kirik et al. 2007) were added to the powder and incubated for 30 min at 4°C (rotating). 100 µl

of the supernatant following centrifugation were mixed with 100 µl 2x Laemmli, boiled for 10 min at 95°C and centrifuged for 1 min at 10 600 g. Samples were separated on SDS-PAGE gels, subsequently blotted and immunodetected (α-GFP (IgG1K, Roche), α-mouse (Jackson ImmunoResearch, www.jacksonimmuno.com)). After GFP detection using the SuperSignal® West Femto Maximum Sensitivity Substrate (ThermoFisher) and a LAS-4000 Mini bioimager (GE Healthcare Life Sciences (formerly Fuji), www.gelifesciences.com), blots were stripped as suggested by Abcam https://www.abcam.com/ps/pdf/protocols/stripping%20for%20reprobing.pdf) using mild stripping buffer (1L: 15 g glycine, 1 g SDS, 10 ml Tween20, pH to 2.2) and re-probed with α-histone H3 (ab1791, Abcam, http://www.abcam.com) and α-rabbit (A6154, Sigma-Aldrich, www.sigmaaldrich.com).

Y2H experiments and Y2H screening. The TTG1pAS2.1-attR construct (Pesch et al. 2015) was used as bait to screen an *A. thaliana* root cDNA library in yeast (Klopffleisch et al. 2011). Y2H screening was performed as described before using 5mM of 3-AT (Soellick & Uhrig 2001). YTH assays were done by co-transformation of pAS2.1-attR/pACT-attR (or TTG1-pcACT2 (Pesch et al. 2015)) vector combination as described previously (Gietz & Schiestl 2007). GFPpAS2.1-attR and GFPpACT (Schrader et al. 2013) served as a negative control. At least three replicates were conducted for each Y2H co-transformation experiment and 6 or 8 individual colonies per transformation were resolved in water in 96-well plates and transferred to SD-LW or SD-LWH plates supplemented with different 3-AT concentrations (3, 5, 10, 15, 20, 30 mM) using a 96-well replica plater. Plates were scanned after one (only SD-LW controlling for successful double transformation and providing a relative comparison of transferred yeast amounts), three and seven days.

Co-localization, microscopy, phenotypic characterization of *ttg1-21* and *ttg1-22*. *Nicothiana benthamiana* leaves were infiltrated as described before (Yang et al. 2000) but using the *Agrobacterium tumefaciens* strain GV3101 pMP90RK harboring the respective constructs and Agrobacteria expressing the silencing suppressor TBSV19K (Voinnet et al. 1999). Infiltrated plants were analyzed three days post-infiltration. CFP-attB1-pBat-TL-B-p35s (this study), YFP-attB1-pBat-TL-B-p35s and RFP-HA-attB1-pBat-TL-B-p35s (Schrader et al. 2013) were used as controls for co-expression with single fluorescent tag fusion protein. The experiment was conducted at least three time for each combination. Infiltrations for the co-expression of CFP and RFP-TTG1 or YFP-TTG1 and RFP, respectively, were included in all experiments. CLSM was performed using a Leica SP8 confocal microscope (Leica Microsystems). Z-stacks were acquired by sequential scanning starting with the laser with the higher wavelength. The LAS Application Suite X (Leica Microsystems) was used to extract and merge images for co-localization figures. Stacks of small leaves acquired as described before (Failmezger et al. 2013) were merged using Combine ZP (by Alan Hadley, https://combinezp.software.informer.com/) for Fig. S1. Pictures of seeds, seedlings and older leaves (14d-old soil and LD grown) were acquired using a stereo

microscope Leica stereomicroscope (MZ FLIII) with the MultiFocus and Montage option of the Leica Application Suite V3 (Leica Microsystems) The step-size was 20 µm (seeds, seedlings) and 50µm (leaves). Seedlings were sterilized as described above and grown on MS (4% sucrose) at constant light at 21 °C.

Data analysis and statistics. All statistics (Table S2, S3, S5), most data analysis, all box plots and plots for qRT-PCR results were generated using R version 3.4.1 (R Core Team 2017) with the following packages: dplyr (Wickham 2019), extrafont (Chang 2014), ggplot2 (Wickham 2009), plyr (Wickham 2011), scales (Wickham 2017), tidyr (Wickham 2018). Schematics for Fig. 1G, S1A and S2 were extracted from CLC DNA Workbench (CLC bio A/S, www.clcbio.com).
Relative protein amounts were determined using fiji (imageJ 1.52h, http://imagej.nih.gov/ij). ROIs of the same size for all bands analyzed within both images of one blot detected with both antibody combinations were measured for their mean grey value intensity. The background close to each band was subtracted, GFP values were set relative to the respective Histone H3 values and values obtained for one blot were normalized to OE01 and - in one case for which OE01 was not evaluated OE20 was used (for OE19-OE21 analysis). Results are shown in Fig. S3.

Results

TTG1 has an effect on flowering time. To date, TTG1 has been analyzed in detail for early (accessible) traits while little is known about its role in the regulation of late developmental traits. When growing *ttg1* mutants, we observed that these flowered slightly earlier than the wild type. Therefore, we selected flowering time - a key late developmental trait - and analyzed classical *ttg1-9* and *ttg1-11* mutants under controlled long-day conditions in the same condition in which the flowering time deviation was monitored first - a comparable warm plant chamber ("warm" condition, on average 23.7°C at the plant's level (chamber set to 22°C), Table S1). Both mutants are in the summer annual Columbia-0 (Col-0) background. We also analyzed flowering time at a slightly reduced temperature (about 2°C less) at long-day conditions ("cold" condition, on average 21.4°C at the plant's level (chamber set to 20°C), Table S1). This can indicate if modifications of the TTG1 protein or modified protein levels might be of adaptive value towards the timing of flowering in dependence of temperature (in different backgrounds) which is suggested by a previous study which identified a SNP in TTG1 having a strong correlation with temperature seasonality, minimum temperature and daylength (Hancock et al. 2011).

We recorded flowering time as the number of days when the first bud was visible and the number of leaves at this timepoint. Both mutants flowered significantly earlier under both conditions (Fig. 1A-B, Table S2). The colder condition revealed that the point mutants *ttg1-9* and *ttg1-11* show differences in their flowering time phenotype: *ttg1-9* exhibited the strongest flowering time phenotype and was only slightly responsive to the difference in temperature as compared to *ttg1-11* and the wild type.

The mutation in the used EMS mutants does not lead to a premature stop codon but change an amino acid. These mutants are known to be no null-mutants at least with respect to their effect on trichome patterning. Therefore, we obtained the recently described additional mutants *ttg1-21* and *ttg1-22* with T-DNA insertions in Col-0 background (Appelhagen et al. 2014; Rosso et al. 2003) causing a premature stop codon within the inserted T-DNA to extend the flowering time analysis. The T-DNA insertion in *ttg1-21* is close to the start before the WD40 domain (Fig. S1A). Therefore, it can be expected that this mutant is a null mutant or at least a comparably strong mutant. In *ttg1-22*, the T-DNA insert is in proximity to the end of TTG1 which might also causes a strong phenotype as seen for the premature stop codon mutant *ttg1-1* in Landsberg *erecta* (L*er*) background. We tested these mutants for some of the early (accessible) TTG1-dependent developmental traits including the so far not reported lack of anthocyanidin accumulation in seedling. When compared to the wild type, the mutants showed the analyzed aspects of the *ttg1* syndrome (Koornneef 1981) similar as observed for the other Col-0 mutants used in this study (Fig. S1). Moreover, we wondered, why the flowering time phenotype of *ttg1* mutants was not reported before. Therefore, we added an often used, classical mutant in L*er* background - *ttg1-1*, a point mutant with a premature stop codon close to the end of TTG1 (Larkin et al. 1994; Walker et al. 1999) - and *ttg1-10,* a mutant in Wassilewskija (Ws) background carrying a point mutation in the *TTG1* promoter (Larkin et al. 1994; Larkin et al. 1999).

The different mutants and variants showed different patterns of flowering time phenotypes in the different accession backgrounds (Fig. 1C-F). Similar to *ttg1-9* and *ttg1-11*, both additional mutants in Col-0 background - *ttg1-21* and *ttg1-22* - flowered significantly earlier in terms of leave number and - with one exception - also in terms of time (days) at our warm and cold condition. For *ttg1-21* grown in the warm condition, the number of days only deviated significantly from the wild type in one out of three repeats and early flowering cannot be concluded in this case.

As flowering time was not significantly reduced in *ttg1-1* as compared to its wild type at both conditions, it is not surprising that the flowering time phenotype was not reported before for this heavily used *ttg1* mutant. The *ttg1-10* mutant carries its mutation in contrast to the other analyzed mutants as a point mutation in its promoter. Interestingly, *ttg1-10* mutants flowered significantly later at both conditions for both recorded flowering phenotypes as compared to its wild type.

For *ttg1-21* and *ttg1-22*, with one exception, it can be summarized that the mutants responded to temperature in the same way as the wild type in regard to time (days) and number of leaves produced until flowering. Only once in three repeats, a significant difference between the results at the two temperatures was recorded for the number of leaves of *ttg1-21* plants at flowering

time. This suggests that these mutants are less responsive to temperature affecting its number of leaves at flowering time as compared to the wild type and *ttg1-22*.

L*er* and *ttg1-1* did not respond to the difference in temperature, when it comes to the number of leaves produced at flowering time. *ttg1-1* and Ws responded only in one out of two experiments to the difference in temperature for the number of days (*ttg1-1*) and leaves (Ws), respectively. In these cases, a reduced response to temperature cannot be concluded. In all other cases, the reduced temperature caused a delay in flowering time as also observed for Col-0 in the other experiments.

As *TTG1-9* and *TTG1-11* encode for TTG1 protein variants, the observed early flowering might be due to a gain- or loss-of-function of the TTG1 variant or *TTG1* gene in the respective mutant. To specify this, we generated overexpression lines of Col-0 TTG1 driven by the constitutively active 35s promoter in Col-0 background (Pro35S::YFP-*TTG1* (Col-0), the three lines are subsequently named OE01-OE03, Fig. 1G). As a regulatory hub in light signaling, COP1 is known to regulate protein stability of relevant flowering time regulators like CO and GI (Jang et al. 2008; Liu et al. 2008; Yu et al. 2008) and is interacting with a *TTG1* gene regulatory network component at the protein level (Maier et al. 2013). Therefore, we included *cop1-4* as a background in the flowering time analysis (Pro35S::YFP-*TTG1* (*cop1-4*), the three lines are subsequently named OE19-OE21).

All overexpression lines in wild-type background flowered late as compared to the wild type at both tested conditions and in respect to time and number of leaves (Fig. 1H-I). This suggests a loss-of-function in the mutant scenario. Compared to Col-0, *cop1-4* produced significantly less leaves at the time point of flowering. An increase in number of leaves and days in this background was only observed for the overexpression line OE20 as compared to its background (Fig. 1H-I). This might be due to different transcript or protein levels in the overexpressors.

In most cases, the overexpression constructs did not affect the endogenous *TTG1* transcript levels. Only in OE19 in *cop1-4* background a significant reduction of endogenous *TTG1* transcript was observed (Fig. 1J, Table S3, see Fig. 1G and Fig. S2 for the selective primer design).

Interestingly, *TTG1* transcript levels were 3-4-fold significantly increased in *cop1-4* mutants as compared to the Col-0 wild type according to both used primer pairs that localized prior to the *TTG1* intron and amplifying the *TTG1* CDS (Fig. 1K-L). All overexpression lines showed a significant overexpression of the construct (Fig. 1K-L). Highest expression and protein levels were reached here by line OE01 in Col-0 background (Fig. 1 K-M, Fig. S3). OE20 (*cop1-4* background) reached the highest expression of the construct and protein level observed in the overexpression lines in *cop1-4* background (Fig. 1K-M, Fig. S3). Both, expression and protein

levels, were consistently at a similar level as for OE02 in the wild-type background. For OE19 and OE21 (*cop1-4* background), similar results were obtained in other repeats being close to or below the detection limit. In Col-0 background, OE03 YFP-TTG1 levels varied the most as compared to the other lines between the repeats which is in agreement with the observation at the fluorescence stereo microscope using older plants. Here, in several OE03 plants YFP-fluorescence was absent in areas of the leaves or in the center of the rosette. This patchiness of YFP fluorescence was also observed in OE21 (*cop1-4* background) and sometimes in OE01 plants (Col-0 background) but only in one out of 50 OE02 plants (Col-0 background) and in none of the OE20 plants (*cop1-4* background) (Table S4). Therefore, and due to the similar transcript and protein level, OE02 and OE20 were chosen for subsequent quantitative RT-PCR (qRT-PCR) experiments.

Together, we revealed that TTG1 has an effect on flowering time. Subsequently, we used q-RT-PCR experiments for an initial embedding of TTG1 in the transcriptional flowering time regulation.

TTG1 can reduce *FT* and *SOC1* transcript levels. *TTG1* acts early in cell fate determination and is a pleiotropic regulator of transcription. The known mechanisms of TTG1 molecular activity are at the protein level at which it acts in differing complex composition with transcription factors that act as the direct modulators of transcription. Therefore, overexpression lines are most informative to initially reveal if the TTG1 protein can have an impact on the transcriptional regulation of specific targets within the individual branches of the flowering time regulatory pathway. All selected targets were analyzed with the most suitable overexpression line as characterized in 2.1.

Moreover, on the one hand, by using the *cop1-4* mutant we added a sensitized background with a significant modulation in protein composition. On the other hand, COP1 interacts with at least one TTG1-complex component (PAP2), therefore, this background also allows for a conclusion if TTG1 activity requires a functional COP1 protein. Results in this background provide insides if TTG1 at elevated protein levels is be able to even overwrite the transcriptional scenario in the light-signaling and LD flowering time mutant *cop1-4*. This would underline even more than in the wild-type scenario the potential adaptive value of TTG1 and relevance as a valuable target for flowering time modulation in various environmental settings.

In addition, for the qRT-PCR experiments of our initial embedding of *TTG1* in the flowering time regulatory pathway, seed material of the two EMS mutants *ttg1-9* and *ttg1-11* was available.

We assessed the circadian expression profile of endogenous and overexpressed *TTG1* in OE02. As for all circadian qRT-PCR experiments in this study, we used 8-day-old LD grown seedlings harvested first at ZT0 and thereafter in intervals of 4 hours with the last sample at ZT20. A

similar overexpression level of *TTG1* was seen throughout the day. The endogenous expression was not affected (see Fig. S4, Table S5).

Due to the strong late flowering phenotype of the overexpression lines, we expected that the transcript levels of the floral integrators (e.g. Blumel et al., 2015) differed from the respective backgrounds. Towards this end, we tested the *CO-FT* module's and *SOC1* transcript levels. In line with the flowering time phenotype, for CO - an activator of *FT* (Suarez-Lopez et al. 2001) - a slight tendency to lower transcript levels in the overexpression lines was observed. Nevertheless, this was neither significant nor sufficient to explain the strong phenotype especially in the overexpression in wild-type background (Fig. 2, Table S5). GI is an *FT* regulator that can increase *CO* transcript levels but can also activate FT in a CO-independent way. It can directly bind to the *FT* promoter and interacts with *FT* suppressors (Sawa & Kay 2011; Sawa et al. 2007). Also, *GI* transcript levels in OE02 were not significantly changed (Fig. S5). In both overexpression lines, for *FT*, the transcript levels almost dropped to the detection limit and exhibited a general reduction at all timepoint which was significant at ZT12 and 16 in OE02. The overexpressors' *SOC1* transcript profiles were very similar in their circadian pattern and both exhibited reductions throughout the day, which was significant at ZT0, 4, 8 and 16 for OE20. In the mutant scenario, we expected to find more subtle effects. We found only a trend to elevated *SOC1* levels in *ttg1-9* mutants which might explain the early flowering time phenotype but was not significant. In summary, we found that TTG1 can reduce *FT* and *SOC1* transcript levels.

Early and late effects on transcript levels of AP2-domain containing factors in *ttg1* mutants.
We moved our focus on factors that suppress *FT* transcript levels, AP2 domain containing factors of the flowering time regulatory pathway: TEM1, TEM2 (RAV transcription factors with AP2/ERF and B3 DNA -binding domain) and AP2, SMZ, SNZ, TOE1-3 e.g. (Song et al. 2013; Wang 2014). In addition, we tested the transcript level of *SVP* which acts as an activator of the AP2-like factors and suppressor of *FT* (Lee et al. 2007; Tao et al. 2012). Only at night, a significant increase of the *TEM2* transcript level was observed for OE02 (Fig. 3, Table S5). No significant change was found for OE20 suggesting that elevated TTG1 levels do not have a strong impact on these genes. However, in the mutants' case a trend for reduced transcript levels was observed for *TEM2* (*ttg1-9*), *AP2*, *TOE1* and *TOE3* (all *ttg1-11*) and a slight reduction for *SNZ* (*ttg1-11*, at night also for *ttg1-9*) and *SMZ* (both mutants). Significance analysis ($P < 0.05$) supported the reduction of *TOE1* transcript levels at ZT4 and ZT16 for *ttg1-11* and *SNZ* transcript levels at ZT20 for *ttg1-9*. Interestingly, although not supported by the significance analysis, the trend of reduced transcript levels for *SVP* seemed to be opposed by elevated *SVP* levels at ZT0 and ZT20 for OE02 pointing to a possibly flattened circadian amplitude of *SVP* transcript levels upon TTG1 overexpression. Therefore, we had a closer look on circadian clock components for OE02.

TTG1 can regulate circadian clock components. LWD1 and LWD2, the closest homologs of TTG1, regulate flowering through transcriptional modulations within the circadian clock (Wang et al. 2011; Wu et al. 2016; Wu et al. 2008). LWD1 was shown to bind to the promoter of *PRR5*, *PRR9* and *PRR1/TOC1* (Wang et al. 2011). Therefore, we analyzed the transcript levels of the core clock components *LHY*, *CCA1* and *TOC1/PRR1* and also those of its feed-back regulators *PRR5*, *PRR7* and *PRR9* (Shim et al. 2017) in the TTG1 overexpression line OE02. Fig. 4 shows the results sorted by the time point of the maximal peak in the wild type. In general, a flattened circadian amplitude is to be seen despite for *TOC1* which is not affected by TTG1 overexpression. For *LHY*, the minimum seems to be shifted to ZT8 instead of ZT12 in the wild type. A significant increase ($P < 0.5$) in transcript levels was observed for *CCA1* at ZT12 and ZT16, *PRR9* at ZT20, *PRR7* at ZT20 and ZT0 and *PRR5* at ZT0 and ZT4. Thus, we found that TTG1 can regulate the transcript levels of circadian clock components and modulates their transcriptional profiles mainly through flattening the amplitude on the day under investigation. Similar as its homologs LWD1 and LWD2, TTG1 can change the transcript levels of *PRRs* but did not modulate *TOC1* transcript levels.

In the transcript levels of the so far analyzed branches of the flowering time regulatory pathway, we did not find a convincing explanation for the strong suppression of *FT* and *SOC1* transcript levels in the overexpression lines. *FLC* represents and integrates additional branches of this pathway. The FLC protein can bind directly to the promoters of *FT* and *SOC1* and suppresses transcript levels (Helliwell et al. 2006; Searle et al. 2006). Therefore, we decided to complete our initial embedding of TTG1 in the transcriptional control of the flowering time pathway by analyzing the transcript levels of *FLC*. We found that overexpression of TTG1 resulted in elevated *FLC* transcript levels throughout the day (Fig. 4). These were significantly and more than 2-fold increased as compared to the wild type at ZT8. We conclude that TTG1 can act as an activator of *FLC*.

One well selected and characterized overexpression line was analyzed in three biological replicates based on three independent seed batches for this initial embedding of TTG1 in the flowering time regulatory pathway. The different and specific time points of transcript modulation spread throughout the day based on the overexpression line OE02 suggest the general ability of TTG1 to elevate transcript levels of clock components and FLC and identify both branches as targets for specific and more detailed follow up studies.
Together we found that TTG1 acts as a transcriptional regulator in various parts of the flowering time regulatory pathway.

PRR5 recruits TTG1 to subnuclear foci and bHLH92 nuclear enrichment is counteracted by TTG1. In its role as a regulator of early (accessible) developmental traits, TTG1 acts through differential complex composition, in competitive scenarios and is for example trapped by the bHLH factor GL3 in the nucleus of developing trichomes (Balkunde et al. 2011; Bouyer et al.

2008; Pesch et al. 2015; Wester et al. 2009; Zhang et al. 2019; Zhang & Schrader 2017; Zhao et al. 2008). All these scenarios occur at the protein level in dependence of its interactors. We wondered, which interactors might be relevant for TTG1 function towards flowering time regulation. As the classical bHLH interactors GL3, EGL3, TT8 and MYC1 did not modulate flowering time in a similar way as TTG1 (Fig. S6), we conducted a Y2H screening to identify candidates which are related to the flowering time regulatory pathway. Among the results of this screen was EGL3 (Table S6), a verified interactor of TTG1 (Zhang et al. 2003). In addition, related to the flowering time regulatory pathway, we identified PRR5 and bHLH92, a bHLH factor shown to be expressed in a circadian pattern (Hanano et al. 2008).

Both selected candidates could be verified as interactors of TTG1 in Y2H experiments in which they were fused to the GAL4-binding as well as to the GAL4-activation domain (Fig. 5A, Fig. S7A-B). We also tested PRR7, PRR9 and TOC1 in the GAL4 system (Fig. 5A) with different 3-AT (3-amino-1,2,3triazole) concentrations and an adjusted optical density of the samples (Fig. S7A-B). All three PRRs interacted with TTG1 when fused to the activation domain of GAL4. TOC1 exhibited the weakest interaction as indicated by growth of yeast on the respective plates followed by PRR9, PRR7 and PRR5. In yeast, the interaction of TTG1 with all PRRs is TTG1-specific. However, a very weak possible interaction of LWD1 and LWD2 was seen with PRR5 in yeast (Fig. S7B-C). bHLH92 did not interact with LWD1, LWD2 and the PRRs in this assay (Fig. S7B-C). This suggests that the mechanisms of LWDs and of the TTG1 protein in flowering time regulation including the transcriptional modification of the circadian clock differ. Here, we continued to focus on the TTG1 protein.

The TTG1 protein is cell-to-cell mobile (Bouyer et al. 2008). Knowing that nuclear trapping by GL3 is a relevant mechanism for TTG1 function in trichome patterning (Balkunde et al. 2011; Bouyer et al. 2008), we analyzed the localization of TTG1 in presence and absence of PRR5 and bHLH92 and vice versa (Fig. 5B-C, Fig. S8-9). As reported before, tagged TTG1 is localized in the cytoplasm and in nucleus in epidermal cells of infiltrated tobacco leaves (e.g. Bouyer et al., 2008). PRR5 is only localized to the nucleus where it forms nuclear foci. When co-expressing RFP-tagged TTG1 and YFP-tagged PRR5, RFP-TTG1 localized predominantly in the nucleus where it co-localized with YFP-PRR5 (Fig. 5B, Fig. S8-9). In case of bHLH92, we obtained a different result. YFP-bHLH92 is enriched in the nucleus but also localizes to the cytoplasm when co-expressed with RFP alone. When co-expressed with RFP-TTG1, TTG1 localization did not change but the nuclear enrichment of bHLH92 did not occur (Fig. 5C, Fig. S8-9). We repeated the experiment with each of the PRRs (PRR5, PRR7, PRR9 and TOC1/PRR1) being fused to CFP in combination with RFP alone or RFP-TTG1 (Fig. 6, Fig. S8-9). The PRRs did not only recruit TTG1 to the nucleus, TTG1 also changed the subnuclear localization for PRR9 and PRR7.

Discussion

TTG1 is a pleiotropic regulator of early (accessible) developmental traits in *A. thaliana*. Here we show, that this view has to be extended as TTG1 also acts later in the plant's life cycle as a regulator of flowering time in *A. thaliana*.

TTG1 variants and protein levels can modulate flowering time. *ttg1* mutants in Col-0 background flowered earlier and overexpressors flowered later at long-day conditions than the Col-0 wild type which is consistent with an observed suppression of *FT* and *SOC1* upon TTG1 overexpression.

Interestingly, the *ttg1-21* mutant, the presumably strongest mutant analyzed in this study due to the very early T-DNA insertion, showed the mildest effect on flowering time as compared to the wildtype. At the warm condition, a significant deviation from the wild type could not be concluded for this mutant in terms of time. This could indicate that the protein's properties - which are presumably changed for the TTG1 variants e.g. concerning their interaction properties - have a stronger effect on flowering time regulation than the reduced level or absence of TTG1. Presence of the TTG1 protein is not required for the plant to flower but elevated levels and variants can modulate flowering time in *A. thaliana*. Therefore, an overexpression line seems to be more beneficial at an early stage to identify targets and interaction partners for TTG1-dependent regulation within the flowering time regulatory pathway to provide the basis for a broad embedding of TTG1 in this pathway. However, the phenotype of the overexpression lines is in agreement with the mutant phenotype of four mutants in the same background and thereby supported by these results. TTG1-dependent regulation through protein level and type of protein variant might follow differing regulatory mechanisms which might be dependent on the respective background and will be of interest to be dissected.

The L*er* wild type was the earliest flowering wild type in our experiment. The *ttg1* mutants did not flower earlier than the wild type with respect to time and number of leaves produced. Therefore, it is not surprising that the flowering phenotype was not reported earlier as the *ttg1-1* has been heavily used in previous studies since the 1980s.

The initially surprising late flowering phenotype of *ttg1-10* in Ws background might be explained by the localization of the mutation within the *TTG1* gene. The *ttg1-10* mutant is an EMS mutant with a point mutation in the *TTG1* promoter. Floral buds did not express the *TTG1* transcript in this mutant (Larkin et al. 1999). This might deviate at different developmental stages and tissues. The mutation might change the expression pattern of TTG1 which in turn can suppress flowering. A manifested second site mutation cannot be excluded as well as an effect of the Ws background.

The relevance of the developmental stage. We acquired data along the chronological and the developmental axis in our flowering time experiments. Results point to an involvement of TTG1 in modulation of the plastochron and detailed meristem analysis at and around the time point of flowering are required in the future.

The relevance of the developmental stage and a possible tissue-specificity might explain why in *ttg1* mutants, *FT* and *SOC1* transcript levels were not significantly increased. In this study, we used 8-day-old LD grown seedlings for the initial embedding of TTG1. As TTG1 is a factor required for cell fate determination (Galway et al. 1994), developmental stage, tissue and cell specific effects might occur. Therefore, older plants and the analysis of tissue specific expression might be required in a more detailed future analysis. This would be of particular relevance for the age pathway and GA signaling which were not cover in this study.

For example, overlaps with the age pathway might occur at the level of the *SQUAMOSA BINDING PROMOTER BINDING PROTEIN-LIKE* (*SPL*)s which are suppressed by microRNA156. SPLs are involved in regulating trichome density at later stages e.g. at the stem (Yu et al. 2010), SPL9 activates *TRIPTYCHON* and *TRICHOMELESS1* and is thought to modulate trichome density thereby (Yu et al. 2010). Both R3-MYBs belong to the so-called inhibitors which compete in the MBW complex scenarios with R2R3-MYBs for bHLH factor binding (Balkunde et al. 2010; Esch et al. 2003; Wang et al. 2008; Wester et al. 2009). TTG1 itself was reported to interact with SPL4 and SPL5 in yeast (Ioannidi et al. 2016) and the mutant of another inhibitor, *enhancer of try and cpc* 3 (*etc3)*, exhibits a differential *FT* and *SOC1* regulation in 21d-old LD-grown plants as compared to the wild type which equals the time of its early flowering time phenotype (Wada & Tominaga-Wada 2015).

FT and SOC1 suppression. If TTG1 acts directly at the *FT* gene, TTG1 can either act directly on the promoter or other regulatory regions of *FT* (and *SOC1*) or affect the *FT* mRNA stability as reported for WERWOLF (WER), a TTG1 network component (Seo et al. 2011). Seo and co-workers found that the mutant of *WER* flowers late and the R2R3-MYB factor WER was revealed to be required for *FT* mRNA stability. It would be interesting to see if this is counteracted by inhibitors like ETC3 or explain the respective phenotypes. Moreover, the role of *WER* towards flowering time regulation was found to be independent of *CO* and *FLC*. Together with our results, the role of TTG1 and WER would be opposing which is not in line with a joined regulation following the classical MBW complexes regulatory mechanisms. However, we can not exclude that *FT* mRNA stability is changed in dependence of TTG1 complexes in parallel to the other observed regulatory effects. By forming an MBW complex with WER, TTG1 could prevent WER from its function towards *FT* mRNA stability which would add to the late flowering time phenotype observed in TTG1 overexpressors.

In our study, we followed the hypothesis that TTG1 acts upstream of *FT*. In this line, if a suppressor of *FT* is regulated by TTG1, it should be suppressed in *ttg1* mutants and increased in the TTG1 overexpressor line with respect to its transcript level. For the mutants and overexpressors, we find a mixed bag of transcript profiles suggesting TTG1 to act in multilayered regulatory mechanisms.

AP2-domain containing factors and the GA signaling branch. With respect to the mutants, indeed, we find several AP2-domain containing factors to exhibit the expected tendencies to reduced transcript levels. However, the overexpressor lines did not show the respective opposing effect. Hence, an intact TTG1 seems to be required for normal circadian transcript profiles of these AP2-domain containing factors.

For TEM1 and TEM2 a connection to the classical TTG1-containing MBW complexes is known. At the transcriptional level, TEM1 and TEM2 act as repressors of the TTG1-MBW complex components GL1, an R2R3-MYB factor, and the bHLH factors GL3 and EGL3 while TTG1 transcript levels are not affected (Matiaz-Hernandez 2016). On the one hand, TEM1 and TEM2 act in a cell type-dependent manner (Matiaz-Hernandez 2016). Therefore, an effect of deviating cell fate and differentiation in the *ttg1* mutants might cause an indirect reduction of the respective transcript level. On the other hand, TEMs control GA accumulation and distribution in the leaf mesophyll. They also integrate the photoperiod and GA signaling pathway in LD and SD conditions (Castillejo and Pelaz, 2008; Matiaz-Hernandez 2016, Osnato et al., 2012). At the molecular level, early flowering in *ttg1-9* with reduced *TEM2* transcript levels might circumvent *FT* and *SOC1* transcript levels. Reduced TEM2 levels lead to elevated GA levels which promote flowering time. However, the late flowering of *ttg1-9* in SD remains obscure. Different binding properties of the mutant protein variant TTG1-9 might cause additional regulatory loops through the GA signaling pathway to play a role. It is known that the bHLH factors GL3, EGL3 and the R2R3-MYB factor GL1, can interact with the DELLA proteins RGA (REPRESSOR OF GA1-3 (mutant of *GA REQUIRING 1*) 1 and RGA2 which both repress the transcriptional activation properties of the MBW complex. This suppression is derepressed by GA through GA-induced degradation of the DELLA proteins (Qi et al. 2014). Also, the discussed inhibitors and the age pathway might play a role combined with the TTG1-9 mutant protein variant.

Competitive scenarios modulating CO protein levels. AP2-domain containing factors can bind directly to the *FT* promoter (Castillejo & Pelaz 2008; Mathieu et al. 2009; Zhang et al. 2015). At the protein level, TOEs can interact with CO and thereby prevent CO from activating *FT* transcription (Zhang et al. 2015). Although a reduction of *CO* transcript levels upon TTG1 overexpression at ZT12 is observed with similarities to the patterns of PRR overexpressors (Hayama et al. 2017), a leading role of CO in the TTG1-dependent regulation of *FT* transcript levels cannot be concluded based on these results. Nevertheless, at the protein level, TTG1 might either decrease CO protein levels or inactivate the CO protein and, thereby, reduce a CO-

mediated *FT* activation. PRRs can stabilize the CO protein (Hayama et al. 2017). Therefore, the interaction of TTG1 with PRRs and re-localization of PRRs, as suggested by our results, could have such an effect which will be tested in the future.

CO protein levels are elevated in *cop1-4* background (Jang et al. 2008). Overexpression of *TTG1* delays flowering time in *cop1-4* background indicating that either the TTG1 protein levels were sufficient to counteract the CO protein function at the protein level or that TTG1 function in the flowering time pathway can be or is mainly independent of CO. However, the effects on flowering time are difficult to compare among wild type and *cop1-4* background as we found increased *TTG1* transcript levels in *cop1-4*.

LWDs, TTG1 and the clock. Further upstream in the photoperiodic pathway, LWD proteins act as activators within the loops of the circadian clock (Shim et al. 2017). It is conceivable that a partial overlap in function exists as these are the two closest homologs of TTG1 in *A. thaliana* but also differences are expected. Towards this end, a detailed evolutionarily focused analysis is of interest.

While *LWD1* transcript levels show a strong circadian response with highest levels late at night and in the long-day morning, *LWD2* and, in our results, *TTG1* do not show this pattern and remain at a similar level during the day and night (Wu et al. 2008). Interestingly, promoter-luciferase constructs showed rhythmic activity of both *LWD* promoters (Wang et al. 2011).

With a focus on LWD1, its binding in a time dependent manner at the promoters of *PRR5, PRR7*, *PRR9* and *CCA1* was revealed (Wang et al. 2011). In *lwd1lwd2* double mutants, *CCA1* and *LHY* transcript levels are reduced, the period is shortened and shifted forward (Wu et al. 2008). In the late afternoon to early morning at LD condition, TTG1 overexpression increases the transcript levels of *PRR5*, *PRR7*, *PRR9*, *CCA1* and *LHY* and potentially reduces the respective transcriptional amplitudes.

A similar mechanism as suggested for CO might occur for CCA1 and LHY. Through binding to the PRRs, these might no longer be able to form a complex with the transcriptional repressors TOPLESS/TOPLESS RELATED PROTEINs (TPL/TPRs) (Wang et al. 2013). Reduced levels or activity of these TPL/TPRs increases *CCA1* and *LHY* transcript levels and lengthen the circadian period (Wang et al. 2013). Similar transcript level characteristics were observed upon TTG1 overexpression in this study apart of the period which was not tested.

LWD1 interacts with TCP transcription factors to activate the expression of CCA1 through binding to the respective promoters (Wang et al. 2011; Wu et al. 2016). Transcriptional activators and repressors interacting with TTG1 might act in comparable regulatory mechanisms mediating target specific DNA-interaction. These need to be embedded into the extended TTG1

network. PRRs and bHLH92 described in this study are excellent candidates. As we did not find strong indications for a clear interaction with LWDs, mechanisms related to PRRs and bHLH92 at the protein level are likely to differ. Being a bHLH factor, bHLH92 might fit well into the regulatory scheme known for TTG1. This would require the identification of an R2R3-MYB interacting with bHLH92. CCA1 and LHY are MYB-like proteins acting as repressors similar to the MBW inhibitors.

TTG1 might act through TTG1-PRR modules. The subnuclear localization patterns upon co-expression of PRRs and bHLH92 with TTG1 provide another potential level of regulation. Do they have an influence on transcriptional activation? What is the identity of the subnuclear foci? Are the interaction partners binding in concert to specific loci, do they stabilize each other, are they stored or deactivated within these foci? These are pressing questions to be answered.

New insights at the protein level will widen our knowledge and interlink known trait networks of the clock, like those of the PRRs, with the TTG1 trait network. For PRR5, target promoters were identified which comprise different transcription factors involved e.g. in auxin production, hypocotyl growth and cold-stress response which might intermingle with growth traits and temperature response observed and expected in TTG1-dependence. Additional evidence for PRRs towards an involvement in growth regulation comes from an antagonistic regulation at the *CDF5* promoter with PIFs. Here, the PRRs suppress hypocotyl elongation from morning to dusk by gating PIF activity. It will be of interest to analyze TTG1-dependent late developmental trait regulation and to identify the respective targets involved to test these for an overlap with clock regulation. TTG1 could overwrite the clock gating when highly abundant in a cell and either regulate through elevate PRR levels an induced growth suppressive effect or, at the protein level, TTG1 might suppress PRR target modulation depending on the relevant downstream targets of both factors at a respective developmental stage.

FT might be such a target as it was shown that a PRR-CDF-FT module can exists. PRR5 can directly suppress CDF expression (Nakamichi et al. 2012) and CDFs can suppress the FT promoter (Song et al. 2012). A TTG1-PRR-CDF-FT module could bypass *GI* and *CO* and could link TTG1 effects on clock gene modulation with *FT* suppression in a competitive scenario with PRR-CDF-FT modules.

A possible parallel TTG1-FLC-FT module. The regulation of flowering time through elevated *FLC* transcript levels in the TTG1 overexpressors appears straight forward. Elevated *FLC* transcript levels lead to an increase in FLC-mediated *FT* and *SOC1* suppression and consequently to late flowering in the overexpression line. In line with this role of TTG1, the weak allele of *FLC* in L*er* background could explain the absence of a flowering time phenotype of the strong *ttg1-1* mutant which has been intensively used in previous studies. It can also explain that the role of TTG1 towards flowering time regulation was not analyzed before. The

TTG1-1 mutant protein variant could not interact with GL3 (Payne et al. 2000) suggesting a high relevance of the C-terminal domain of TTG1 towards protein-protein interaction presumably at the level of the protein structure. All used accessions in this study are rapid cycling accessions lacking a functional FRI allele and therefore immediately exposing modulations at *FLC* to potential phenotypic detection.

Overlapping regulatory network. The annual plant *A. thaliana* completes its life cycle with the production and ripening of seeds and enters the new life cycle following seed dormancy with seed germination. The reproductive success depends therefore on the appropriate timing of flowering and seed ripening as well as germination thereafter. Therefore, it is not surprising that a pleiotropic regulator like TTG1 which is strongly involved in the regulation of various relevant seed traits, is also involved in the regulation of flowering time. Here, it is noteworthy that TTG1-dependent gene regulatory network components including TTG1 have the potential to intervene in several sub-pathways of flowering time regulation. We found that TTG1 can even overwrite the transcriptional scenario in *cop1-4* in regard to the floral integrators FT and SOC1. Moreover, TTG1 variants are likely to be of relevance in adaptation to temperature seasonality, minimum temperature and daylength (Hancock et al. 2011). This strongly suggests an adaptive value of the TTG1-dependent trait network which is strengthened by the overlapping gene regulatory networks of TTG1 and flowering time regulation substantiated through this study.

Conclusions

Plants can respond to endogenous and exogenous cues through concerted regulation of specific trait networks. Pleiotropic regulators can aid to reveal such trait networks of adaptive value. The pleiotropic regulator *TRANSPARENT TESTA GLABRA 1* is known as head of a conserved gene regulatory network regulating early accessible developmental traits. Surprisingly little has been known about its involvement in late developmental trait regulation. We reveal that TTG1 is a flowering time regulator in *Arabidopsis thaliana* and provide an initial embedding in the flowering time regulatory pathway. TTG1 modulates transcript levels of key elements within this pathway - the floral integrators *FT* and *SOC1*. We show that TTG1 might act upstream of *FLC* and the circadian clock. At the protein level we found differential interdependencies with regard to the subcellular and subnuclear localization of clock proteins and TTG1 *in planta*. In summary, our results provide an initial embedding of TTG1 in the flowering time regulatory pathway. This will allow for an informed in depth embeddings within the individual branches of the flowering time regulatory pathway and a future analysis of overlapping trait networks of adaptive value.

Acknowledgements

The authors thank Martin Hülskamp (University of Cologne) for hosting and financing A.S. and this work. We thank Alexander Schurz for laboratory and plant work assistance, Iqra Javed for a tobacco infiltration and support with yeast work, Julian Schiffner for “TTG1 both” qRT-PCR primers, Sabine Lohmer for maintenance of the yeast strain and Bastian Welter for technical

assistance while cloning CFPattB1-pBat-TL-p35s. We are grateful to the following persons for providing seeds and plasmids: Martin Hülskamp providing access to his lab stock, Martina Pesch for bHLH vectors used for cloning, George Coupland (Liron Sarid-Krebs/Brigitte Koop) (Max Planck Institute for Plant Breeding Research, Germany) for 35S::PRR7:CFP and 35S::PRR9:CFP and Martin Sagasser/Bernd Weisshaar (Center for Biotechnology, University of Bielefeld, Germany) for *ttg1-21* and *ttg1-22*. We wish to thank Klaus Menrath (University of Cologne) and his team for perfect plant care and providing tobacco plants. Last but not least we wish to thank for all constructive contributions within the reviewing process.

References

Alonso JM, Stepanova AN, Leisse TJ, Kim CJ, Chen H, Shinn P, Stevenson DK, Zimmerman J, Barajas P, Cheuk R, Gadrinab C, Heller C, Jeske A, Koesema E, Meyers CC, Parker H, Prednis L, Ansari Y, Choy N, Deen H, Geralt M, Hazari N, Hom E, Karnes M, Mulholland C, Ndubaku R, Schmidt I, Guzman P, Aguilar-Henonin L, Schmid M, Weigel D, Carter DE, Marchand T, Risseeuw E, Brogden D, Zeko A, Crosby WL, Berry CC, and Ecker JR. 2003. Genome-wide insertional mutagenesis of Arabidopsis thaliana. *Science* 301:653-657. 10.1126/science.1086391

An H, Roussot C, Suarez-Lopez P, Corbesier L, Vincent C, Pineiro M, Hepworth S, Mouradov A, Justin S, Turnbull C, and Coupland G. 2004. CONSTANS acts in the phloem to regulate a systemic signal that induces photoperiodic flowering of Arabidopsis. *Development* 131:3615-3626. 10.1242/dev.01231

Andres F, and Coupland G. 2012. The genetic basis of flowering responses to seasonal cues. *Nat Rev Genet* 13:627-639. 10.1038/nrg3291

Appelhagen I, Jahns O, Bartelniewoehner L, Sagasser M, Weisshaar B, and Stracke R. 2011. Leucoanthocyanidin Dioxygenase in Arabidopsis thaliana: characterization of mutant alleles and regulation by MYB-BHLH-TTG1 transcription factor complexes. *Gene* 484:61-68. 10.1016/j.gene.2011.05.031

Appelhagen I, Thiedig K, Nordholt N, Schmidt N, Huep G, Sagasser M, and Weisshaar B. 2014. Update on transparent testa mutants from Arabidopsis thaliana: characterisation of new alleles from an isogenic collection. *Planta* 240:955-970. 10.1007/s00425-014-2088-0

Balasubramanian S, Sureshkumar S, Lempe J, and Weigel D. 2006. Potent induction of Arabidopsis thaliana flowering by elevated growth temperature. *PLoS Genet* 2:e106. 10.1371/journal.pgen.0020106

Balkunde R, Bouyer D, and Hulskamp M. 2011. Nuclear trapping by GL3 controls intercellular transport and redistribution of TTG1 protein in Arabidopsis. *Development* 138:5039-5048. 10.1242/dev.072454

Balkunde R, Pesch M, and Hulskamp M. 2010. Trichome patterning in Arabidopsis thaliana from genetic to molecular models. *Current Topics in Developmental Biology* 91:299-321. 10.1016/S0070-2153(10)91010-7

Blazquez MA, Ahn JH, and Weigel D. 2003. A thermosensory pathway controlling flowering time in Arabidopsis thaliana. *Nat Genet* 33:168-171. 10.1038/ng1085

Blumel M, Dally N, and Jung C. 2015. Flowering time regulation in crops-what did we learn from Arabidopsis? *Curr Opin Biotechnol* 32:121-129. 10.1016/j.copbio.2014.11.023

Bouyer D, Geier F, Kragler F, Schnittger A, Pesch M, Wester K, Balkunde R, Timmer J, Fleck C, and Hulskamp M. 2008. Two-dimensional patterning by a trapping/depletion mechanism: the role of TTG1 and GL3 in Arabidopsis trichome formation. *PLoS Biol* 6:e141. 10.1371/journal.pbio.0060141

Broun P. 2005. Transcriptional control of flavonoid biosynthesis: a complex network of conserved regulators involved in multiple aspects of differentiation in Arabidopsis. *Curr Opin Plant Biol* 8:272-279. 10.1016/j.pbi.2005.03.006

Castillejo C, and Pelaz S. 2008. The balance between CONSTANS and TEMPRANILLO activities determines FT expression to trigger flowering. *Curr Biol* 18:1338-1343. 10.1016/j.cub.2008.07.075

Chang W. 2014. extrafont: Tools for using fonts. R package version 0.17.

Chen M, Zhang B, Li C, Kulaveerasingam H, Chew FT, and Yu H. 2015. TRANSPARENT TESTA GLABRA1 Regulates the Accumulation of Seed Storage Reserves in Arabidopsis. *Plant Physiol* 169:391-402. 10.1104/pp.15.00943

Clough SJ, and Bent AF. 1998. Floral dip: a simplified method for Agrobacterium-mediated transformation of Arabidopsis thaliana. *Plant J* 16:735-743.

Deng X, Qiu Q, He K, and Cao X. 2018. The seekers: how epigenetic modifying enzymes find their hidden genomic targets in Arabidopsis. *Curr Opin Plant Biol* 45:75-81. 10.1016/j.pbi.2018.05.006

Dodd AN, Salathia N, Hall A, Kevei E, Toth R, Nagy F, Hibberd JM, Millar AJ, and Webb AA. 2005. Plant circadian clocks increase photosynthesis, growth, survival, and competitive advantage. *Science* 309:630-633. 10.1126/science.1115581

Esch JJ, Chen M, Sanders M, Hillestad M, Ndkium S, Idelkope B, Neizer J, and Marks MD. 2003. A contradictory GLABRA3 allele helps define gene interactions controlling trichome development in Arabidopsis. *Development* 130:5885-5894. 10.1242/dev.00812

Failmezger H, Jaegle B, Schrader A, Hulskamp M, and Tresch A. 2013. Semi-automated 3D Leaf Reconstruction and Analysis of Trichome Patterning from Light Microscopic Images. *PLoS Comput Biol* 9:e1003029. 10.1371/journal.pcbi.1003029

Feys BJ, Wiermer M, Bhat RA, Moisan LJ, Medina-Escobar N, Neu C, Cabral A, and Parker JE. 2005. Arabidopsis SENESCENCE-ASSOCIATED GENE101 stabilizes and signals within an ENHANCED DISEASE SUSCEPTIBILITY1 complex in plant innate immunity. *Plant Cell* 17:2601-2613. 10.1105/tpc.105.033910

Galway ME, Masucci JD, Lloyd AM, Walbot V, Davis RW, and Schiefelbein JW. 1994. The TTG gene is required to specify epidermal cell fate and cell patterning in the Arabidopsis root. *Dev Biol* 166:740-754. 10.1006/dbio.1994.1352

Gietz RD, and Schiestl RH. 2007. High-efficiency yeast transformation using the LiAc/SS carrier DNA/PEG method. *Nat Protoc* 2:31-34. 10.1038/nprot.2007.13

Grigorova B, Mara C, Hollender C, Sijacic P, Chen X, and Liu Z. 2011. LEUNIG and SEUSS co-repressors regulate miR172 expression in Arabidopsis flowers. *Development* 138:2451-2456. 10.1242/dev.058362

Hanano S, Stracke R, Jakoby M, Merkle T, Domagalska MA, Weisshaar B, and Davis SJ. 2008. A systematic survey in Arabidopsis thaliana of transcription factors that modulate circadian parameters. *BMC Genomics* 9:182. 10.1186/1471-2164-9-182

Hancock AM, Brachi B, Faure N, Horton MW, Jarymowycz LB, Sperone FG, Toomajian C, Roux F, and Bergelson J. 2011. Adaptation to climate across the Arabidopsis thaliana genome. *Science* 334:83-86. 10.1126/science.1209244

Harari-Steinberg O, Ohad I, and Chamovitz DA. 2001. Dissection of the light signal transduction pathways regulating the two early light-induced protein genes in Arabidopsis. *Plant Physiol* 127:986-997.

Hayama R, Sarid-Krebs L, Richter R, Fernandez V, Jang S, and Coupland G. 2017. PSEUDO RESPONSE REGULATORs stabilize CONSTANS protein to promote flowering in response to day length. *EMBO J* 36:904-918. 10.15252/embj.201693907

Helliwell CA, Wood CC, Robertson M, James Peacock W, and Dennis ES. 2006. The Arabidopsis FLC protein interacts directly in vivo with SOC1 and FT chromatin and is

970 part of a high-molecular-weight protein complex. *Plant J* 46:183-192. 10.1111/j.1365-
971 313X.2006.02686.x
972 Hepworth J, and Dean C. 2015. Flowering Locus C's Lessons: Conserved Chromatin Switches
973 Underpinning Developmental Timing and Adaptation. *Plant Physiol* 168:1237-1245.
974 10.1104/pp.15.00496
975 Huang H, and Nusinow DA. 2016. Into the Evening: Complex Interactions in the Arabidopsis
976 Circadian Clock. *Trends Genet* 32:674-686. 10.1016/j.tig.2016.08.002
977 Ioannidi E, Rigas S, Tsitsekian D, Daras G, Alatzas A, Makris A, Tanou G, Argiriou A,
978 Alexandrou D, Poethig S, Hatzopoulos P, and Kanellis AK. 2016. Trichome patterning
979 control involves TTG1 interaction with SPL transcription factors. *Plant Mol Biol* 92:675-
980 687. 10.1007/s11103-016-0538-8
981 Jaegle B, Uroic MK, Holtkotte X, Lucas C, Termath AO, Schmalz HG, Bucher M, Hoecker U,
982 Hulskamp M, and Schrader A. 2016. A fast and simple LC-MS-based characterization of
983 the flavonoid biosynthesis pathway for few seed(ling)s. *BMC Plant Biol* 16:190.
984 10.1186/s12870-016-0880-7
985 Jakoby MJ, Falkenhan D, Mader MT, Brininstool G, Wischnitzki E, Platz N, Hudson A,
986 Hulskamp M, Larkin J, and Schnittger A. 2008. Transcriptional profiling of mature
987 Arabidopsis trichomes reveals that NOECK encodes the MIXTA-like transcriptional
988 regulator MYB106. *Plant Physiol* 148:1583-1602. 10.1104/pp.108.126979
989 Jang S, Marchal V, Panigrahi KC, Wenkel S, Soppe W, Deng XW, Valverde F, and Coupland G.
990 2008. Arabidopsis COP1 shapes the temporal pattern of CO accumulation conferring a
991 photoperiodic flowering response. *EMBO J* 27:1277-1288. 10.1038/emboj.2008.68
992 Kirik V, Schrader A, Uhrig JF, and Hulskamp M. 2007. MIDGET unravels functions of the
993 Arabidopsis topoisomerase VI complex in DNA endoreduplication, chromatin
994 condensation, and transcriptional silencing. *Plant Cell* 19:3100-3110.
995 10.1105/tpc.107.054361
996 Klopffleisch K, Phan N, Augustin K, Bayne RS, Booker KS, Botella JR, Carpita NC, Carr T,
997 Chen JG, Cooke TR, Frick-Cheng A, Friedman EJ, Fulk B, Hahn MG, Jiang K, Jorda L,
998 Kruppe L, Liu C, Lorek J, McCann MC, Molina A, Moriyama EN, Mukhtar MS, Mudgil Y,
999 Pattathil S, Schwarz J, Seta S, Tan M, Temp U, Trusov Y, Urano D, Welter B, Yang J,
1000 Panstruga R, Uhrig JF, and Jones AM. 2011. Arabidopsis G-protein interactome reveals
1001 connections to cell wall carbohydrates and morphogenesis. *Mol Syst Biol* 7:532.
1002 10.1038/msb.2011.66
1003 Koornneef M. 1981. The complex syndrome of ttg mutants. *Arabidopsis Information Service*
1004 18:45-51.
1005 Koornneef M, and Meinke D. 2010. The development of Arabidopsis as a model plant. *Plant J*
1006 61:909-921. 10.1111/j.1365-313X.2009.04086.x
1007 Larkin JC, Oppenheimer DG, Lloyd AM, Paparozzi ET, and Marks MD. 1994. Roles of the
1008 GLABROUS1 and TRANSPARENT TESTA GLABRA Genes in Arabidopsis Trichome
1009 Development. *Plant Cell* 6:1065-1076. 10.1105/tpc.6.8.1065
1010 Larkin JC, Walker JD, Bolognesi-Winfield AC, Gray JC, and Walker AR. 1999. Allele-specific
1011 interactions between ttg and gl1 during trichome development in Arabidopsis thaliana.
1012 *Genetics* 151:1591-1604.
1013 Laubinger S, Marchal V, Le Gourrierec J, Wenkel S, Adrian J, Jang S, Kulajta C, Braun H,
1014 Coupland G, and Hoecker U. 2006. Arabidopsis SPA proteins regulate photoperiodic
1015 flowering and interact with the floral inducer CONSTANS to regulate its stability.
1016 *Development* 133:3213-3222. 10.1242/dev.02481
1017 Lee J, and Lee I. 2010. Regulation and function of SOC1, a flowering pathway integrator. *J Exp*
1018 *Bot* 61:2247-2254. 10.1093/jxb/erq098

1019 Lee JH, Yoo SJ, Park SH, Hwang I, Lee JS, and Ahn JH. 2007. Role of SVP in the control of
1020 flowering time by ambient temperature in Arabidopsis. *Genes Dev* 21:397-402.
1021 10.1101/gad.1518407
1022 Lepiniec L, Debeaujon I, Routaboul JM, Baudry A, Pourcel L, Nesi N, and Caboche M. 2006.
1023 Genetics and biochemistry of seed flavonoids. *Annu Rev Plant Biol* 57:405-430.
1024 10.1146/annurev.arplant.57.032905.105252
1025 Li C, Zhang B, Chen B, Ji L, and Yu H. 2018. Site-specific phosphorylation of TRANSPARENT
1026 TESTA GLABRA1 mediates carbon partitioning in Arabidopsis seeds. *Nat Commun*
1027 9:571. 10.1038/s41467-018-03013-5
1028 Li D, Liu C, Shen L, Wu Y, Chen H, Robertson M, Helliwell CA, Ito T, Meyerowitz E, and Yu H.
1029 2008. A repressor complex governs the integration of flowering signals in Arabidopsis.
1030 *Dev Cell* 15:110-120. 10.1016/j.devcel.2008.05.002
1031 Liu LJ, Zhang YC, Li QH, Sang Y, Mao J, Lian HL, Wang L, and Yang HQ. 2008. COP1-
1032 mediated ubiquitination of CONSTANS is implicated in cryptochrome regulation of
1033 flowering in Arabidopsis. *Plant Cell* 20:292-306. 10.1105/tpc.107.057281
1034 Locke JC, Kozma-Bognar L, Gould PD, Feher B, Kevei E, Nagy F, Turner MS, Hall A, and Millar
1035 AJ. 2006. Experimental validation of a predicted feedback loop in the multi-oscillator
1036 clock of Arabidopsis thaliana. *Mol Syst Biol* 2:59. 10.1038/msb4100102
1037 Maier A, Schrader A, Kokkelink L, Falke C, Welter B, Iniesto E, Rubio V, Uhrig JF, Hulskamp M,
1038 and Hoecker U. 2013. Light and the E3 ubiquitin ligase COP1/SPA control the protein
1039 stability of the MYB transcription factors PAP1 and PAP2 involved in anthocyanin
1040 accumulation in Arabidopsis. *Plant J* 74:638-651. 10.1111/tpj.12153
1041 Makino S, Kiba T, Imamura A, Hanaki N, Nakamura A, Suzuki T, Taniguchi M, Ueguchi C,
1042 Sugiyama T, and Mizuno T. 2000. Genes encoding pseudo-response regulators: insight
1043 into His-to-Asp phosphorelay and circadian rhythm in Arabidopsis thaliana. *Plant Cell*
1044 *Physiol* 41:791-803. 10.1093/pcp/41.6.791
1045 Martel F, Grundemann D, and Schomig E. 2002. A simple method for elimination of false
1046 positive results in RT-PCR. *J Biochem Mol Biol* 35:248-250.
1047 Mathieu J, Yant LJ, Murdter F, Kuttner F, and Schmid M. 2009. Repression of flowering by the
1048 miR172 target SMZ. *PLoS Biol* 7:e1000148. 10.1371/journal.pbio.1000148
1049 Matsushika A, Makino S, Kojima M, and Mizuno T. 2000. Circadian waves of expression of the
1050 APRR1/TOC1 family of pseudo-response regulators in Arabidopsis thaliana: insight into
1051 the plant circadian clock. *Plant Cell Physiol* 41:1002-1012. 10.1093/pcp/pcd043
1052 McNellis TW, von Arnim AG, Araki T, Komeda Y, Misera S, and Deng XW. 1994. Genetic and
1053 molecular analysis of an allelic series of cop1 mutants suggests functional roles for the
1054 multiple protein domains. *Plant Cell* 6:487-500. 10.1105/tpc.6.4.487
1055 Michael TP, Salome PA, Yu HJ, Spencer TR, Sharp EL, McPeek MA, Alonso JM, Ecker JR, and
1056 McClung CR. 2003. Enhanced fitness conferred by naturally occurring variation in the
1057 circadian clock. *Science* 302:1049-1053. 10.1126/science.1082971
1058 Michaels SD, He Y, Scortecci KC, and Amasino RM. 2003. Attenuation of FLOWERING LOCUS
1059 C activity as a mechanism for the evolution of summer-annual flowering behavior in
1060 Arabidopsis. *Proc Natl Acad Sci U S A* 100:10102-10107. 10.1073/pnas.1531467100
1061 Miller JC, Chezem WR, and Clay NK. 2015. Ternary WD40 Repeat-Containing Protein
1062 Complexes: Evolution, Composition and Roles in Plant Immunity. *Front Plant Sci* 6:1108.
1063 10.3389/fpls.2015.01108
1064 Nakamichi N, Kiba T, Henriques R, Mizuno T, Chua NH, and Sakakibara H. 2010. PSEUDO-
1065 RESPONSE REGULATORS 9, 7, and 5 are transcriptional repressors in the Arabidopsis
1066 circadian clock. *Plant Cell* 22:594-605. 10.1105/tpc.109.072892
1067 Nakamichi N, Kiba T, Kamioka M, Suzuki T, Yamashino T, Higashiyama T, Sakakibara H, and
1068 Mizuno T. 2012. Transcriptional repressor PRR5 directly regulates clock-output
1069 pathways. *Proc Natl Acad Sci U S A* 109:17123-17128. 10.1073/pnas.1205156109

1070 Nakamichi N, Kita M, Niinuma K, Ito S, Yamashino T, Mizoguchi T, and Mizuno T. 2007.
1071 Arabidopsis clock-associated pseudo-response regulators PRR9, PRR7 and PRR5
1072 coordinately and positively regulate flowering time through the canonical CONSTANS-
1073 dependent photoperiodic pathway. *Plant Cell Physiol* 48:822-832. 10.1093/pcp/pcm056
1074 Neff MM, Turk E, and Kalishman M. 2002. Web-based primer design for single nucleotide
1075 polymorphism analysis. *Trends Genet* 18:613-615.
1076 Oakenfull RJ, and Davis SJ. 2017. Shining a light on the Arabidopsis circadian clock. *Plant Cell*
1077 *Environ* 40:2571-2585. 10.1111/pce.13033
1078 Osnato M, Castillejo C, Matias-Hernandez L, and Pelaz S. 2012. TEMPRANILLO genes link
1079 photoperiod and gibberellin pathways to control flowering in Arabidopsis. *Nat Commun*
1080 3:808. 10.1038/ncomms1810
1081 Payne CT, Zhang F, and Lloyd AM. 2000. GL3 encodes a bHLH protein that regulates trichome
1082 development in arabidopsis through interaction with GL1 and TTG1. *Genetics* 156:1349-
1083 1362.
1084 Pesch M, Schultheiss I, Digiuni S, Uhrig JF, and Hulskamp M. 2013. Mutual control of
1085 intracellular localisation of the patterning proteins AtMYC1, GL1 and TRY/CPC in
1086 Arabidopsis. *Development* 140:3456-3467. 10.1242/dev.094698
1087 Pesch M, Schultheiss I, Klopffleisch K, Uhrig JF, Koegl M, Clemen CS, Simon R, Weidtkamp-
1088 Peters S, and Hulskamp M. 2015. TRANSPARENT TESTA GLABRA1 and GLABRA1
1089 Compete for Binding to GLABRA3 in Arabidopsis. *Plant Physiol* 168:584-597.
1090 10.1104/pp.15.00328
1091 Qi T, Huang H, Wu D, Yan J, Qi Y, Song S, and Xie D. 2014. Arabidopsis DELLA and JAZ
1092 proteins bind the WD-repeat/bHLH/MYB complex to modulate gibberellin and jasmonate
1093 signaling synergy. *Plant Cell* 26:1118-1133. 10.1105/tpc.113.121731
1094 R Core Team. 2017. R: A Language and Environment for Statistical Computing. Vienna,
1095 Austria: R Foundation for Statistical Computing.
1096 Ramsay NA, and Glover BJ. 2005. MYB-bHLH-WD40 protein complex and the evolution of
1097 cellular diversity. *Trends Plant Sci* 10:63-70. 10.1016/j.tplants.2004.12.011
1098 Rosso MG, Li Y, Strizhov N, Reiss B, Dekker K, and Weisshaar B. 2003. An Arabidopsis
1099 thaliana T-DNA mutagenized population (GABI-Kat) for flanking sequence tag-based
1100 reverse genetics. *Plant Mol Biol* 53:247-259. 10.1023/B:PLAN.0000009297.37235.4a
1101 Sawa M, and Kay SA. 2011. GIGANTEA directly activates Flowering Locus T in Arabidopsis
1102 thaliana. *Proc Natl Acad Sci U S A* 108:11698-11703. 10.1073/pnas.1106771108
1103 Sawa M, Nusinow DA, Kay SA, and Imaizumi T. 2007. FKF1 and GIGANTEA complex
1104 formation is required for day-length measurement in Arabidopsis. *Science* 318:261-265.
1105 10.1126/science.1146994
1106 Schrader A, Welter B, Hulskamp M, Hoecker U, and Uhrig JF. 2013. MIDGET connects COP1-
1107 dependent development with endoreduplication in Arabidopsis thaliana. *Plant J* 75:67-
1108 79. 10.1111/tpj.12199
1109 Searle I, He Y, Turck F, Vincent C, Fornara F, Krober S, Amasino RA, and Coupland G. 2006.
1110 The transcription factor FLC confers a flowering response to vernalization by repressing
1111 meristem competence and systemic signaling in Arabidopsis. *Genes Dev* 20:898-912.
1112 10.1101/gad.373506
1113 Seo E, Yu J, Ryu KH, Lee MM, and Lee I. 2011. WEREWOLF, a regulator of root hair pattern
1114 formation, controls flowering time through the regulation of FT mRNA stability. *Plant*
1115 *Physiol* 156:1867-1877. 10.1104/pp.111.176685
1116 Shim JS, Kubota A, and Imaizumi T. 2017. Circadian Clock and Photoperiodic Flowering in
1117 Arabidopsis: CONSTANS Is a Hub for Signal Integration. *Plant Physiol* 173:5-15.
1118 10.1104/pp.16.01327

1119 Shin J, Sanchez-Villarreal A, Davis AM, Du SX, Berendzen KW, Koncz C, Ding Z, Li C, and
1120 Davis SJ. 2017. The metabolic sensor AKIN10 modulates the Arabidopsis circadian
1121 clock in a light-dependent manner. *Plant Cell Environ* 40:997-1008. 10.1111/pce.12903
1122 Simpson GG, and Dean C. 2002. Arabidopsis, the Rosetta stone of flowering time? *Science*
1123 296:285-289. 10.1126/science.296.5566.285
1124 Soellick TR, and Uhrig JF. 2001. Development of an optimized interaction-mating protocol for
1125 large-scale yeast two-hybrid analyses. *Genome Biol* 2:RESEARCH0052.
1126 Song YH, Ito S, and Imaizumi T. 2013. Flowering time regulation: photoperiod- and
1127 temperature-sensing in leaves. *Trends Plant Sci* 18:575-583.
1128 10.1016/j.tplants.2013.05.003
1129 Song YH, Shim JS, Kinmonth-Schultz HA, and Imaizumi T. 2015. Photoperiodic flowering: time
1130 measurement mechanisms in leaves. *Annu Rev Plant Biol* 66:441-464.
1131 10.1146/annurev-arplant-043014-115555
1132 Song YH, Smith RW, To BJ, Millar AJ, and Imaizumi T. 2012. FKF1 conveys timing information
1133 for CONSTANS stabilization in photoperiodic flowering. *Science* 336:1045-1049.
1134 10.1126/science.1219644
1135 Strayer C, Oyama T, Schultz TF, Raman R, Somers DE, Mas P, Panda S, Kreps JA, and Kay
1136 SA. 2000. Cloning of the Arabidopsis clock gene TOC1, an autoregulatory response
1137 regulator homolog. *Science* 289:768-771.
1138 Suarez-Lopez P, Wheatley K, Robson F, Onouchi H, Valverde F, and Coupland G. 2001.
1139 CONSTANS mediates between the circadian clock and the control of flowering in
1140 Arabidopsis. *Nature* 410:1116-1120. 10.1038/35074138
1141 Sun CW, and Callis J. 1997. Independent modulation of Arabidopsis thaliana polyubiquitin
1142 mRNAs in different organs and in response to environmental changes. *Plant J* 11:1017-
1143 1027.
1144 Tao Z, Shen L, Liu C, Liu L, Yan Y, and Yu H. 2012. Genome-wide identification of SOC1 and
1145 SVP targets during the floral transition in Arabidopsis. *Plant J* 70:549-561.
1146 10.1111/j.1365-313X.2012.04919.x
1147 Tominaga-Wada R, Ishida T, and Wada T. 2011. New insights into the mechanism of
1148 development of Arabidopsis root hairs and trichomes. *Int Rev Cell Mol Biol* 286:67-106.
1149 10.1016/B978-0-12-385859-7.00002-1
1150 Turck F, Fornara F, and Coupland G. 2008. Regulation and identity of florigen: FLOWERING
1151 LOCUS T moves center stage. *Annu Rev Plant Biol* 59:573-594.
1152 10.1146/annurev.arplant.59.032607.092755
1153 Valverde F, Mouradov A, Soppe W, Ravenscroft D, Samach A, and Coupland G. 2004.
1154 Photoreceptor regulation of CONSTANS protein in photoperiodic flowering. *Science*
1155 303:1003-1006. 10.1126/science.1091761
1156 Voinnet O, Pinto YM, and Baulcombe DC. 1999. Suppression of gene silencing: a general
1157 strategy used by diverse DNA and RNA viruses of plants. *Proc Natl Acad Sci U S A*
1158 96:14147-14152.
1159 Wada T, and Tominaga-Wada R. 2015. CAPRICE family genes control flowering time through
1160 both promoting and repressing CONSTANS and FLOWERING LOCUS T expression.
1161 *Plant Sci* 241:260-265. 10.1016/j.plantsci.2015.10.015
1162 Walker AR, Davison PA, Bolognesi-Winfield AC, James CM, Srinivasan N, Blundell TL, Esch JJ,
1163 Marks MD, and Gray JC. 1999. The TRANSPARENT TESTA GLABRA1 locus, which
1164 regulates trichome differentiation and anthocyanin biosynthesis in Arabidopsis, encodes
1165 a WD40 repeat protein. *Plant Cell* 11:1337-1350. 10.1105/tpc.11.7.1337
1166 Wang CQ, Guthrie C, Sarmast MK, and Dehesh K. 2014. BBX19 interacts with CONSTANS to
1167 repress FLOWERING LOCUS T transcription, defining a flowering time checkpoint in
1168 Arabidopsis. *Plant Cell* 26:3589-3602. 10.1105/tpc.114.130252

Wang JW. 2014. Regulation of flowering time by the miR156-mediated age pathway. *J Exp Bot* 65:4723-4730. 10.1093/jxb/eru246

Wang L, Kim J, and Somers DE. 2013. Transcriptional corepressor TOPLESS complexes with pseudoresponse regulator proteins and histone deacetylases to regulate circadian transcription. *Proc Natl Acad Sci U S A* 110:761-766. 10.1073/pnas.1215010110

Wang S, Hubbard L, Chang Y, Guo J, Schiefelbein J, and Chen JG. 2008. Comprehensive analysis of single-repeat R3 MYB proteins in epidermal cell patterning and their transcriptional regulation in Arabidopsis. *BMC Plant Biol* 8:81. 10.1186/1471-2229-8-81

Wang Y, Wu JF, Nakamichi N, Sakakibara H, Nam HG, and Wu SH. 2011. LIGHT-REGULATED WD1 and PSEUDO-RESPONSE REGULATOR9 form a positive feedback regulatory loop in the Arabidopsis circadian clock. *Plant Cell* 23:486-498. 10.1105/tpc.110.081661

Wenden B, Kozma-Bognar L, Edwards KD, Hall AJ, Locke JC, and Millar AJ. 2011. Light inputs shape the Arabidopsis circadian system. *Plant J* 66:480-491. 10.1111/j.1365-313X.2011.04505.x

Wester K, Digiuni S, Geier F, Timmer J, Fleck C, and Hulskamp M. 2009. Functional diversity of R3 single-repeat genes in trichome development. *Development* 136:1487-1496. 10.1242/dev.021733

Wickham H. 2009. *Ggplot2 : elegant graphics for data analysis*. New York: Springer.

Wickham H. 2011. The Split-Apply-Combine Strategy for Data Analysis. *Journal of Statistical Software* 40:1--29.

Wickham H. 2017. scales: Scale Functions for Visualization. R package version 0.5.0.

Wickham HaH, L. 2018. tidyr: Easily Tidy Data with 'spread()' and 'gather()' Functions. R package version 0.8.0.

Wickham HF, R. ; Henry, L. and Müller, K. . 2019. dplyr: A Grammar of Data Manipulation. R package version 0.8.0.1.

Wu JF, Tsai HL, Joanito I, Wu YC, Chang CW, Li YH, Wang Y, Hong JC, Chu JW, Hsu CP, and Wu SH. 2016. LWD-TCP complex activates the morning gene CCA1 in Arabidopsis. *Nat Commun* 7:13181. 10.1038/ncomms13181

Wu JF, Wang Y, and Wu SH. 2008. Two new clock proteins, LWD1 and LWD2, regulate Arabidopsis photoperiodic flowering. *Plant Physiol* 148:948-959. 10.1104/pp.108.124917

Yang Y, Li R, and Qi M. 2000. In vivo analysis of plant promoters and transcription factors by agroinfiltration of tobacco leaves. *Plant J* 22:543-551.

Yant L, Mathieu J, and Schmid M. 2009. Just say no: floral repressors help Arabidopsis bide the time. *Curr Opin Plant Biol* 12:580-586. 10.1016/j.pbi.2009.07.006

Yu JW, Rubio V, Lee NY, Bai S, Lee SY, Kim SS, Liu L, Zhang Y, Irigoyen ML, Sullivan JA, Zhang Y, Lee I, Xie Q, Paek NC, and Deng XW. 2008. COP1 and ELF3 control circadian function and photoperiodic flowering by regulating GI stability. *Mol Cell* 32:617-630. 10.1016/j.molcel.2008.09.026

Yu N, Cai WJ, Wang S, Shan CM, Wang LJ, and Chen XY. 2010. Temporal control of trichome distribution by microRNA156-targeted SPL genes in Arabidopsis thaliana. *Plant Cell* 22:2322-2335. 10.1105/tpc.109.072579

Yu S, Galvao VC, Zhang YC, Horrer D, Zhang TQ, Hao YH, Feng YQ, Wang S, Schmid M, and Wang JW. 2012. Gibberellin regulates the Arabidopsis floral transition through miR156-targeted SQUAMOSA promoter binding-like transcription factors. *Plant Cell* 24:3320-3332. 10.1105/tpc.112.101014

Zhang B, Chopra D, Schrader A, and Hülskamp M. 2019. Evolutionary comparison of competitive protein-complex formation of MYB, bHLH, and WDR proteins in plants. *Journal of Experimental Botany*. 10.1093/jxb/erz155

Zhang B, and Schrader A. 2017. TRANSPARENT TESTA GLABRA 1-Dependent Regulation of Flavonoid Biosynthesis. *Plants (Basel)* 6. 10.3390/plants6040065

Zhang B, Wang L, Zeng L, Zhang C, and Ma H. 2015. Arabidopsis TOE proteins convey a photoperiodic signal to antagonize CONSTANS and regulate flowering time. *Genes Dev* 29:975-987. 10.1101/gad.251520.114

Zhang F, Gonzalez A, Zhao M, Payne CT, and Lloyd A. 2003. A network of redundant bHLH proteins functions in all TTG1-dependent pathways of Arabidopsis. *Development* 130:4859-4869. 10.1242/dev.00681

Zhao M, Morohashi K, Hatlestad G, Grotewold E, and Lloyd A. 2008. The TTG1-bHLH-MYB complex controls trichome cell fate and patterning through direct targeting of regulatory loci. *Development* 135:1991-1999. 10.1242/dev.016873

Zou Y, Wang Y, Wang L, Yang L, Wang R, and Li X. 2013. miR172b controls the transition to autotrophic development inhibited by ABA in Arabidopsis. *PLoS One* 8:e64770. 10.1371/journal.pone.0064770

Figure 1

TTG1 has an effect on flowering time regulation in the *A. thaliana* Col-0 ecotype at long-day conditions.

(A-D) Flowering time of *ttg1* mutants in Col-0 background. In **(A-F,H,I)**, flowering time was recorded as the number of days until bolting **(A,C,E,H)** or the number of leaves at the time-point of bolting **(B,D,F,I)**. Plants were grown at long-day conditions (16h light, 8h darkness) at 21°C ("cold") or 23°C ("warm"). Black lines in the box plots represent the median, red dots are the mean for the shown representative experiment and crosses mark outliers. Asterisks indicate significant differences (*P < 0.05) between the mutants and the Col-0 wild type (orange) or between the two conditions (grey) in the shown representative experiment. Numbers in brackets indicate the number of experiments for which a significant difference was observed out of the total number of experiments. **(G)** Primer binding sites for the used primer pairs for qRT-PCR (arrow heads) relative to the *TTG1* genomic, cDNA, CDS and overexpression construct sequence. The position of the point mutations in the *ttg1-9* and *ttg1-11* is indicated above. The T-DNA insertion for *ttg1-21* and *ttg1-22* are provided in Fig. S1 characterizing the mutants' phenotypes. See Fig. S2 for an alignment of *TTG1* with *LWD1* and *LWD2* in the primer binding region. The sense primers for the primer pairs "TTG both" and "TTG1 no LWD" are overlapping and the sequence of the latter deviates at its 3' end from the sequence for LWD1 and LWD2. The name "TTG1 both" indicates that the CDS as well as the construct are amplified by this primer pair. **(H,I)** Flowering time of *TTG1* overexpression lines as described above. **(J-M)** Characterization of transcript and protein levels in lines overexpressing YFP-*TTG1* in Col-0 (OE01-03) and *cop1-4* (OE19-21) background driven by the 35S promoter. **(J-L)** Highest levels of *TTG1* transcript were observed in OE01-03 (Col-0) and OE20 (*cop1-4*) while the endogenous *TTG1* transcript levels were in general not affected by overexpression despite in the OE19 (*cop1-4*) line. Note the elevated

TTG1 levels in *cop1-4* mutants. Transcript levels were determined by qRT-PCR relative to *UBQ10* using 8-day-old seedlings and are normalized with Col-0 wild type values. Data represent the mean of three independent experiments. Asterisks indicate significant differences (#: $P < 0.1$, *: $P < 0.05$) between overexpression lines and the backgrounds Col-0 (orange) and *cop1-4* (magenta), respectively. Please note that the scale in **(K,L)** differs from the scale in **(J)**. The solid line equals 1. The y-axis is in $\log_{10}$-scaled. Error bars indicate the SD. **(M)** Western blot using 7d-old long-day grown seedlings form one of the repeats used in (J-L). In OE03 (Col-0), YFP-TTG1 levels varied between experiments never exceeding those in OE01 (Col-0). See also Fig. S3. Tables S2-4 provide more details on the underlying data and statistics. OE01-03: Pro35s:YFP-*TTG1* (Col-0), three independent insertion lines. OE19-21: Pro35s:YFP-*TTG1* (*cop1-4*), three independent insertion lines.

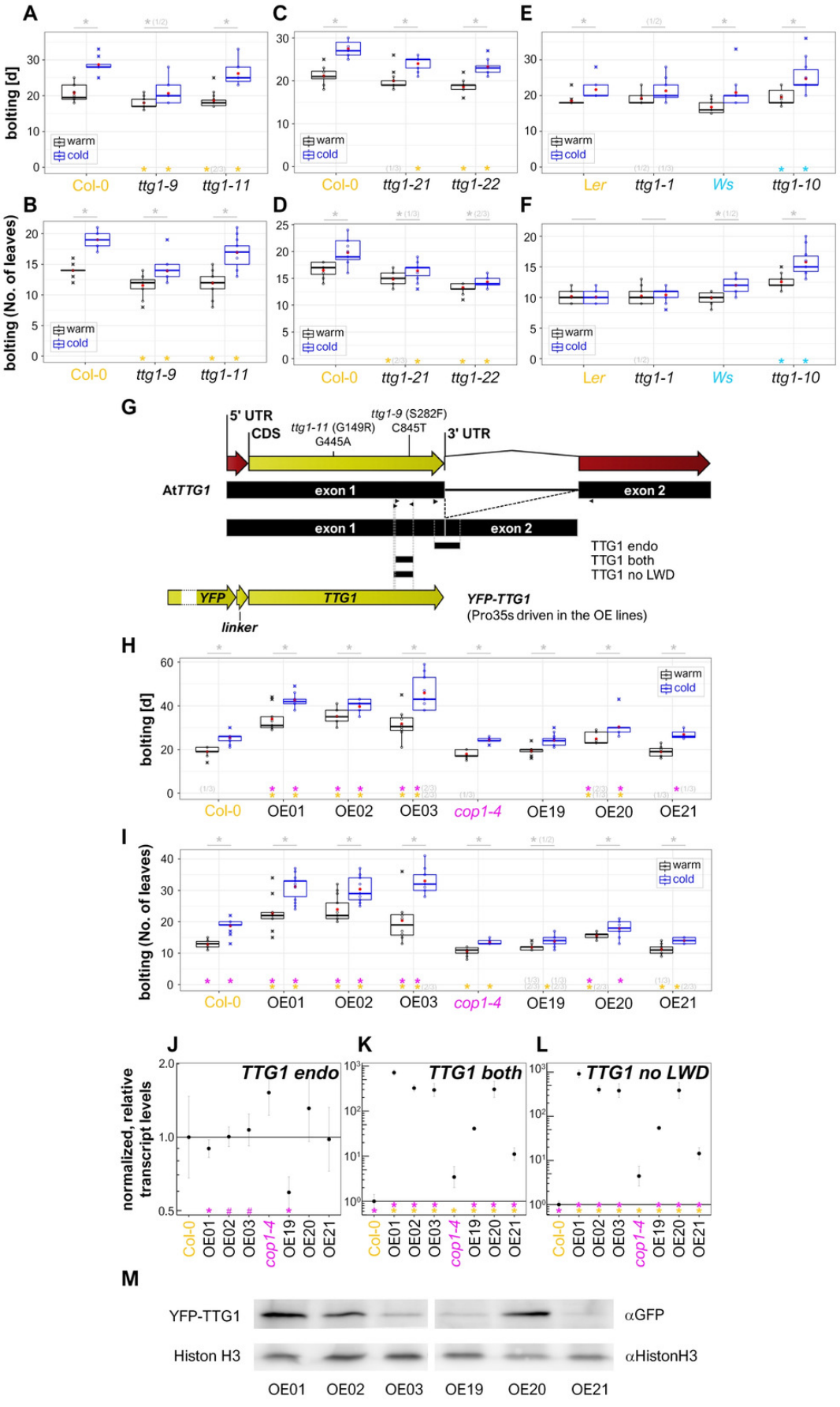

Figure 2

TTG1 overexpression suppresses *FT* and *SOC1* transcript levels which can not be explained by *CO* transcript levels.

(A-D) Eight-day-old seedlings grown under LD conditions (light: ZT0-16, dark: ZT16-0) at 21°C were harvested in 4h-intervals starting at ZT0. The analyzed genotypes were *ttg1* mutants in Col-0 background, TTG1 overexpression lines in Col-0 (OE02) and in *cop1-4* (OE20) background with their respective backgrounds. *CO*, *FT* and *SOC1* transcript levels were analyzed. Transcript levels are presented relative to the *UBQ10* transcript levels and normalized with the maximal mean per target within a genotype set. (E-G) Same growth conditions as used for A-D. The seedlings were harvested at ZT=11 and ZT=13 from OE01-03 (Pro35s:YFP-*TTG1* (Col-0), three independent insertion lines) and OE19-21 (Pro35s:YFP-*TTG1* (*cop1-4*), three independent insertion lines), Col-0 and *cop1-4*. Data are means from three biological replicates originating from three independent seed batches (A-D) or from one seed batch of parallely grown parental plants (E-G). Error bars are SD. Asterisks indicate significant differences (#P < 0.1, *P < 0.05) between the mutants (blue: *ttg1-9*, cyan: *ttg1-11*) and their background or the overexpression lines and their respective backgrounds Col-0 (orange) and *cop1-4* (magenta). Dashed line: averaged lower threshold in the set of experiments for the respective target (Ct=35) relative to the respective *UBQ10* levels. Dotted line: average lower threshold + SD. The solid line equals 1. The y-axis is $\log_{10}$-scaled. See Table S3 for more details on the underlying data and statistics.

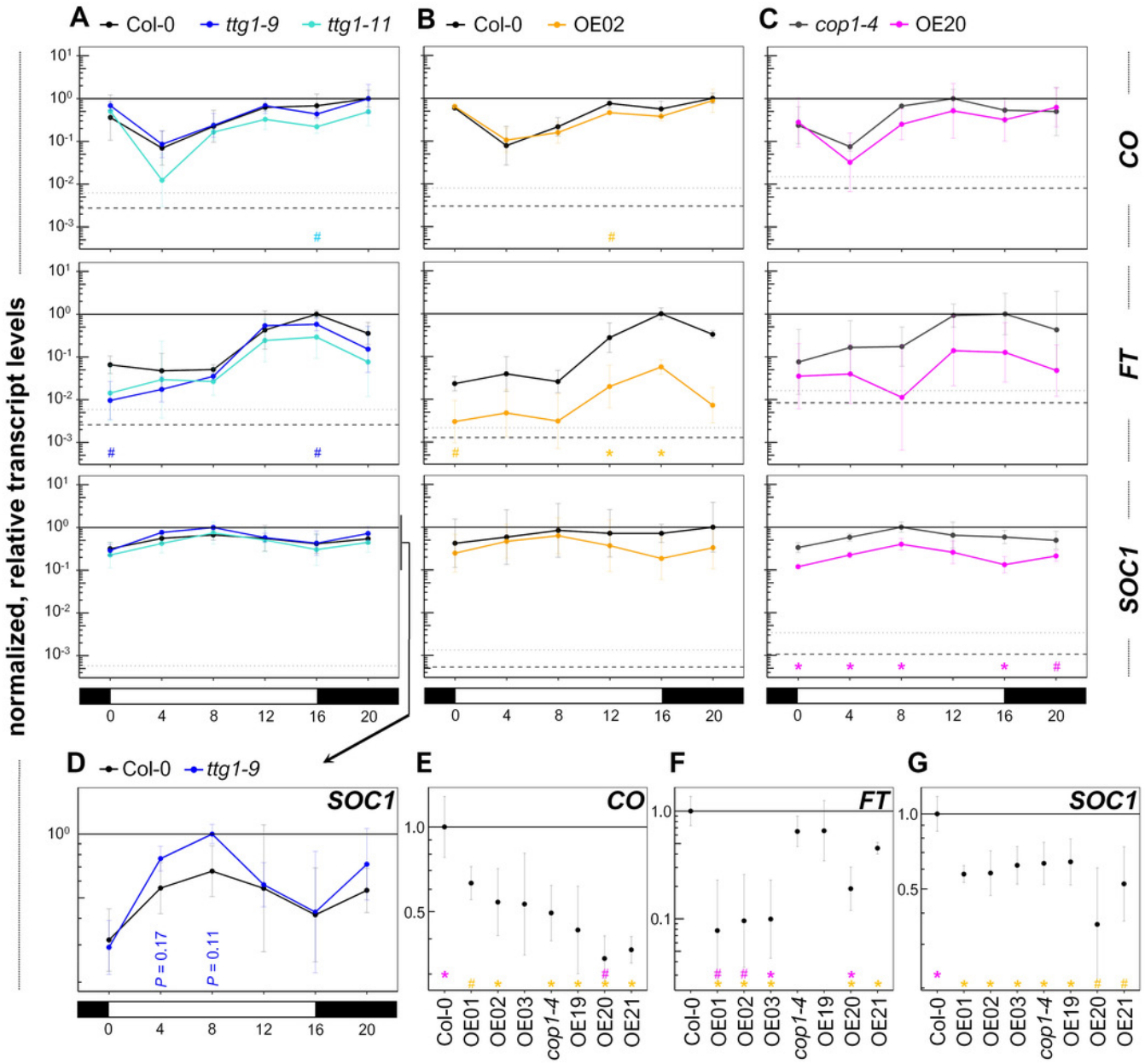

Figure 3

AP2-domain containing factors: Reduction of *TEM2*, *SNZ, TOE1* and *TOE3* transcript levels in *ttg1* mutants occurs early and late under long-day conditions.

In the mutants and overexpressors, we analyzed the transcript levels of transcriptional *FT* suppressors: AP2 family genes *AP2*, *SMZ*, *SNZ*, *TOE1*, *TOE2*, *TOE3,* the two RAV factors *TEM1* and *TEM2* as well as *SVP*, an activator of AP2 family genes and suppressor of *FT*. The same samples as in Fig. 2 were used. Data are means from three biological replicates. Error bars are SD. Dotted line: average lower threshold in the set of experiments for the respective target (Ct=35) relative to the respective *UBQ10* levels + SD. The solid line equals 1. The y-axis is in $\log_{10}$-scaled. For details on the genotypes and data presentation please refer to Fig. 2 and for details on the underlying data and statistics to Table S5.

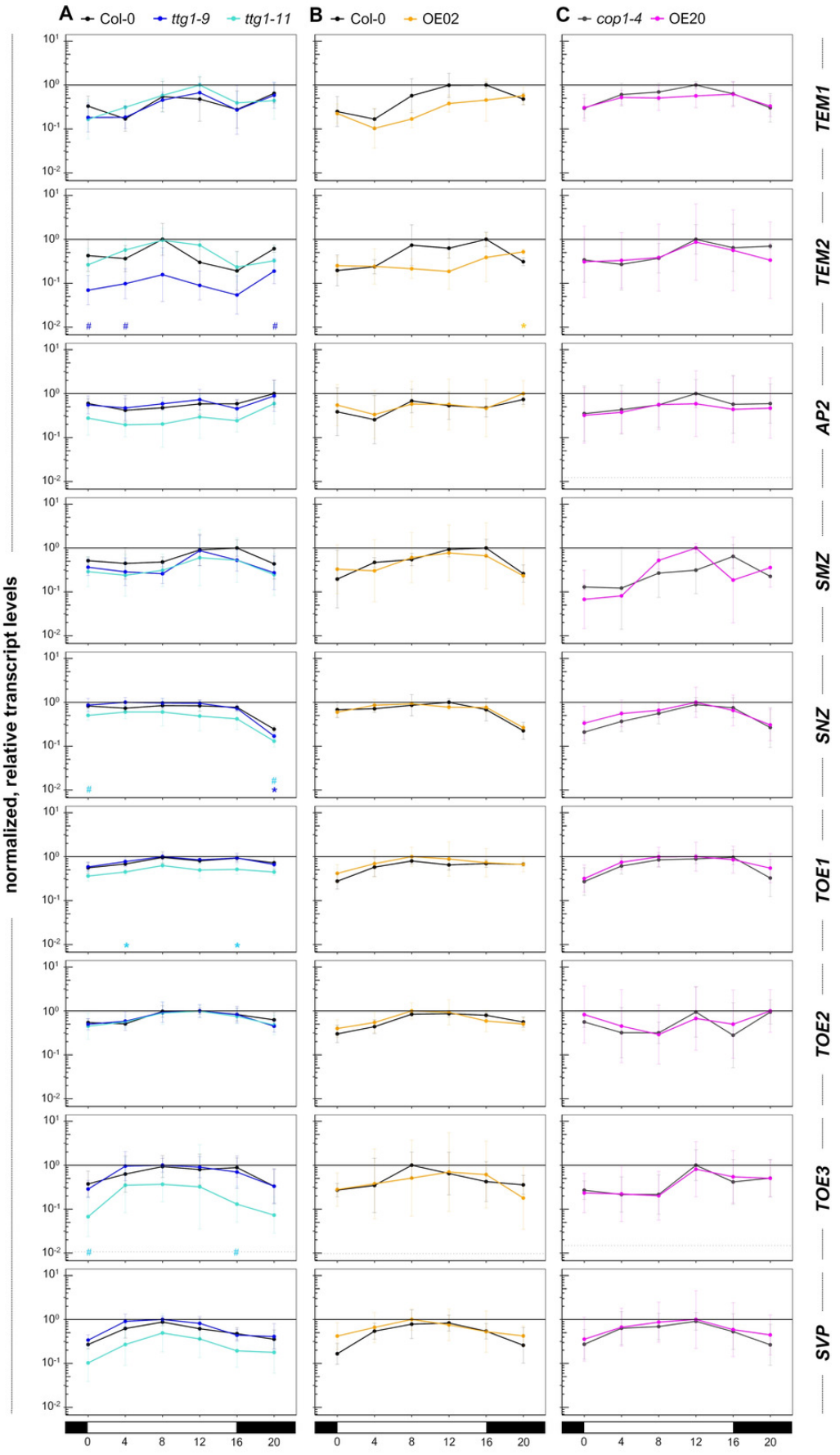

Figure 4

TTG1 can modulate transcript levels of circadian clock components, flattens their circadian amplitude and *TTG1* overexpression increases *FLC* transcript levels.

To further explore an additional relevant part of the flowering time regulatory pathway, we used the overexpression line in Col-0 background to analyze eight-day-old seedlings grown under LD conditions (light: ZT0-16, dark: ZT16-0) at 21°C which were harvested in 4h-intervals starting at ZT0. The analyzed clock components are sorted according to their peak during the day. The selected overexpression line in Col-0 background (OE02) was also employed to further explore another relevant FT-suppressive branch of the flowering time regulatory pathway: FLC transcript levels. Transcript levels are relative to that of *UBQ10* and normalized with the maximal mean per target. Data are means from three biological replicates. Error bars are SD. Asterisks indicate significant differences (*P < 0.05) between the overexpression line and the Col-0 wild type. Dashed line: averaged lower threshold in the set of experiments for the respective target (Ct=35) relative to the respective *UBQ10* levels. Dotted line: average lower threshold + SD. The solid line equals 1. The y-axis is in $\log_{10}$-scaled. See Table S5 for more details on the underlying data and statistics.

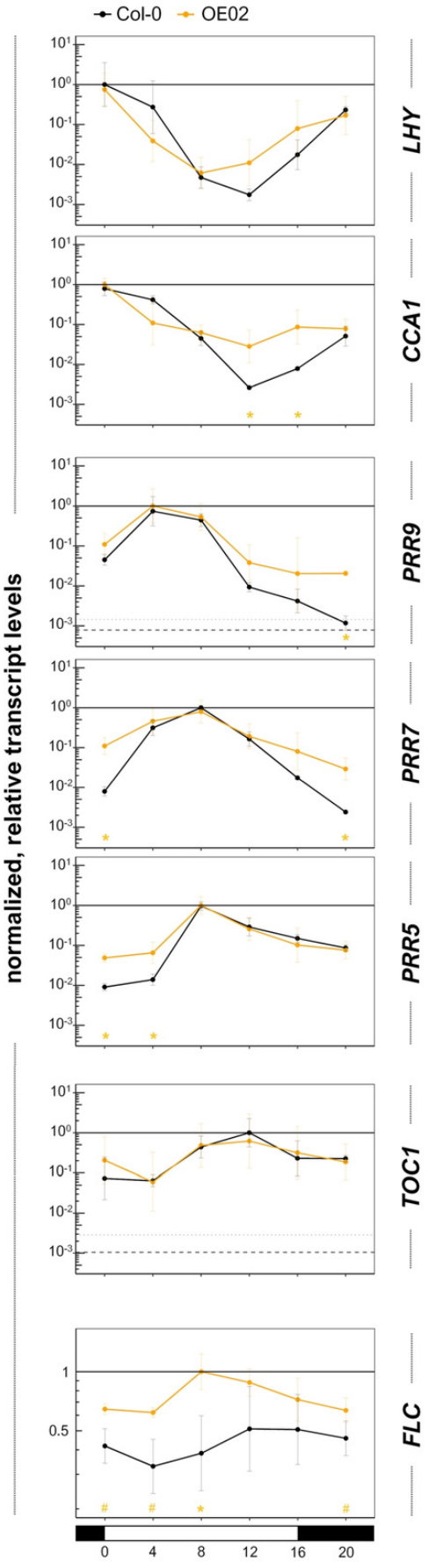

Figure 5

TTG1 interacts with PRR5 and bHLH92 in yeast with suggested functional relevance due to protein re-localizations *in planta*.

(A) Yeast two-hybrid assay with TTG1 as a bait (A1). TTG1 was tested for interaction with the PRRs (TOC1/PRR1, PRR5, PRR7, PRR9) and bHLH92. GFP serves as a negative control (A2). Yeast colonies were transferred to interaction plates (SD-LWH) and plates to test for successful co-transformation (SD-LW). Interaction plates were supplemented with different 3-AT concentrations: 3, 5, 10, 15, 20, 30 mM to qualitatively assess differences in interaction strength. See Fig. S7 for additional results discussed in the text. AD = GAL4-activation domain; BD = GAL4-DNA-binding domain (used for bait constructs); SD = synthetic defined medium. **(B-C)** Representative sequentially scanned, merged confocal stacks of *N. benthamiana* leaf epidermal cells co-expressing RFP- and YFP- (B) or CFP- tagged (C) proteins. **(B)** YFP-TTG1 is recruited by RFP-PRR5 to subnuclear foci. Constructs were co-infiltrated to co-express YFP-TTG1 and RFP (B1-3), YFP and RFP-PRR5 (B4-6) or YFP-TTG1 and RFP-PRR5 (B(7-9) as also indicated above each column. The indicated channels (left of the respective row) were subsequently merged (B3,6,9) and no brightness-contrast correction was applied. Please note that we did neither differentially adjust the detection nor the pictures for YFP among the combinations to improve visualization of the faint YFP-TTG1 signal in order to visualize the strong effect of RFP-PRR5 on YFP-TTG1 protein localization and abundance within the nucleus (B7). **(C)** Enrichment of CFP-bHLH92 in the nucleus is reduced when RFP-TTG1 is co-expressed. Constructs were co-infiltrated to co-express CFP and RFP-TTG1 (C1-3), CFP-bHLH92 and RFP (C4-6) and CFP-bHLH92 and RFP-TTG1 (C7-10) as also indicated above each column. C1,4,7-8 show infiltrated leaf areas of the indicated tagged protein in the respective channel. The same post-acquisition brightness and contrast adjustment was applied to all pictures marked with „adj“ (C1,3-5,7-10). White arrows point to

representative nuclei with differing, relative CFP-bHL92 enrichment as compared to the cytoplasm and in dependence on the presence of RFP-TTG1. All pictures within (B) and within (C) were acquired with the same settings for RFP/YFP and RFP/CFP, respectively, despite for a reduced laser intensity for the RFP detection of the CFP-bHLH92/RFP combination (C6) and a smaller image size for the CFP/RFP-TTG1 combination (C2-3) (512x512 as compared to 2058x2058 px²). In Fig. S9 we provide adjusted and non-adjusted pictures for RFP-TTG1 to visualize the protein‘s localization. See also Fig. 6 for CFP-PRR/RFP-TTG1 combinations. Bars equal 100 µm in the leaf area pictures and 50 µm in all other pictures. Additional confocal images are shown in Fig. S8-9. All experiments in the figure were at least conducted three times independently with the same results.

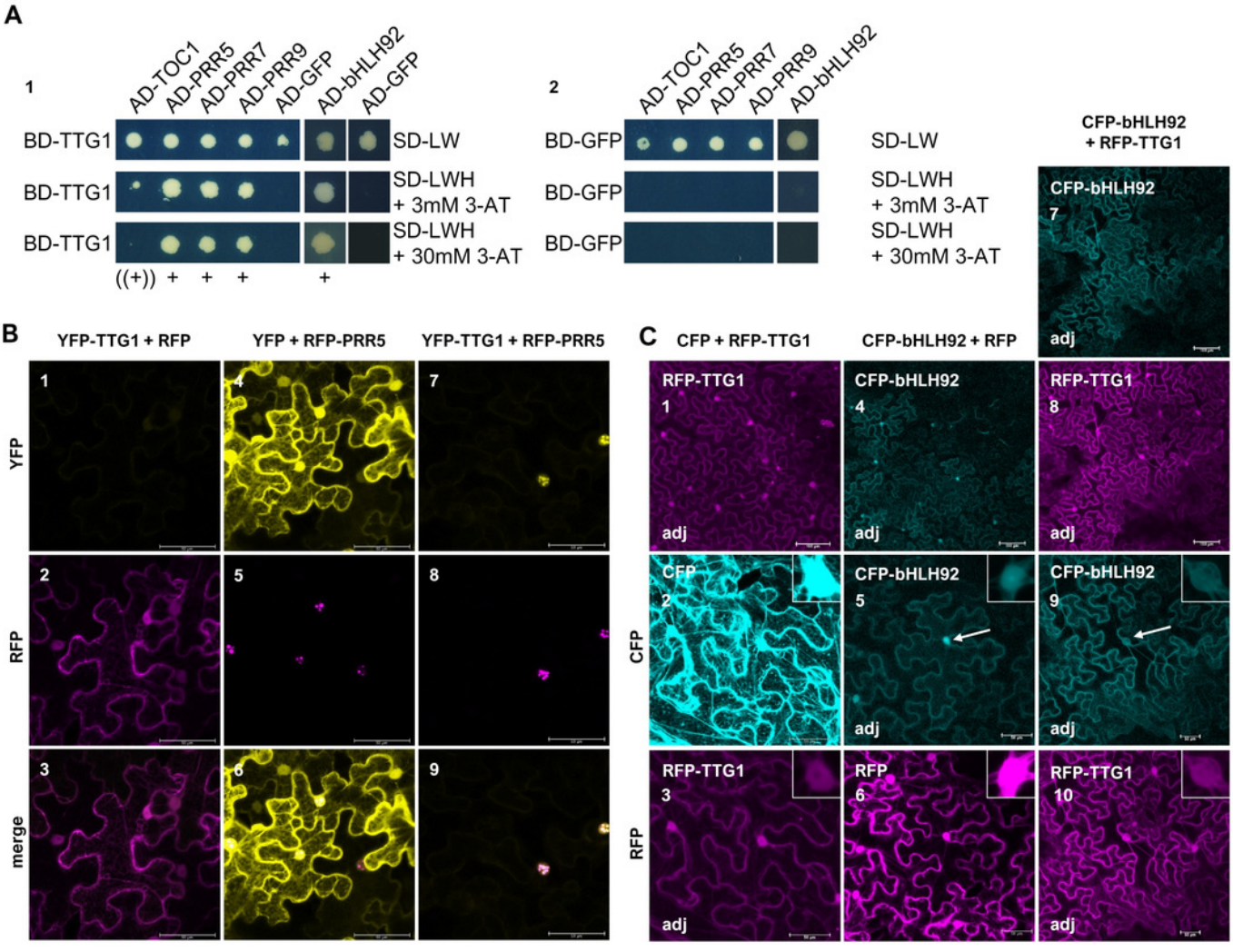

Figure 6

PRRs can re-localize TTG1 to different distinct (sub-)nuclear localizations.

Representative sequentially scanned, merged confocal stacks of *N. benthamiana* leaf epidermal cells. Combinations of RFP-TTG1 or RFP with CFP-PRR and CFP given above each column were co-expressed. The indicated channels were subsequently merged and a brightness-contrast correction was only applied in the second upper column for the CFP/RFP-TTG1 combination to visualize RFP-TTG1 presence and localization. Insets show representative observed nuclear localization. Please note that for CFP-PRR7/RFP (and to a minor extend for CFP-TOC1/RFP-TTG1) different subnuclear localizations were seen in all three experiments conducted and that the subnuclear localization of PRR9 and PRR7 was also modified by RFP-TTG1. White arrows in the CFP-PRR7/RFP picture point to week CFP fluorescing nuclei without intense subnuclear foci. These were not dominant but present. For the CFP-TOC1/RFP-TTG1 combination, arrowheads in the left inset of a characteristic nucleus point to faint subnuclear foci into which RFP-TTG1 is recruited. Pictures of all nuclei including bars which are shown here as insets are shown in Fig. S8. Orange box: Non-adjusted pictures of the RFP channel detection for co-infiltrations of RFP-TTG1 with CFP or CFP-tagged PRRs showing an area of the respective leave. See also Fig. S9 for pictures with increased brightness and contrast. Bars equal 50µm for representative cells and 100 µm for the leaf areas.